1 The strigolactone receptor D14 targets SMAX1 for degradation in response to GR24 2 treatment and osmotic stress 3 4 Qingtian Li¹, Elena Sánchez Martín-Fontecha², Aashima Khosla¹, Alexandra R.F. White¹, Sunhyun Chang¹, Pilar Cubas², David C. Nelson^{1C} 5 6 7 ¹Department of Botany and Plant Sciences, University of California, Riverside, CA 8 92521 USA 9 10 ²Plant Molecular Genetics Department, Centro Nacional de Biotecnología/CSIC, 11 Campus Universidad Autónoma de Madrid, Madrid, Spain 12 13 ^cCorresponding author, david.nelson@ucr.edu 14 15 Running title: Crosstalk between D14 and SMAX1 16 17 Keywords: phytohormone, signaling, proteolysis, crosstalk 18 The author(s) responsible for distribution of materials integral to the findings presented 19 20 in this article is: David C. Nelson (david.nelson@ucr.edu).

ABSTRACT

21

The phytohormone strigolactone (SL) and smoke-derived karrikins (KARs) have mostly 22 23 distinct effects on plants despite being perceived through very similar mechanisms. The homologous receptors DWARF14 (D14) and KARRIKIN INSENSITIVE2 (KAI2) mediate 24 25 SL and KAR responses, respectively, with the F-box protein MORE AXILLARY GROWTH2 (MAX2) by targeting different SMAX1-LIKE (SMXL) family proteins for 26 27 degradation. These mechanisms are putatively well-insulated, with D14-MAX2 targeting SMXL6, SMXL7, and SMXL8, and KAI2-MAX2 targeting SMAX1 and SMXL2 in 28 29 Arabidopsis thaliana. Recent evidence challenges this model. We investigated whether D14 can target SMAX1 and whether this occurs naturally. Genetic analysis indicates the 30 31 SL analog GR24 promotes D14-SMAX1 crosstalk. Although D14 shows weaker interactions with SMAX1 than SMXL2 or SMXL7, D14 mediates GR24-induced 32 33 degradation of SMAX1 in plants. Osmotic stress triggers SMAX1 degradation, which is protective, through SL biosynthesis and signaling genes. Thus, D14-SMAX1 crosstalk 34 35 may be beneficial and not simply a vestige of the SL pathway's evolution.

INTRODUCTION

36

Strigolactones (SLs) and karrikins (KARs) are two classes of butenolide molecules that 37 38 regulate diverse aspects of plant development. SLs were discovered in root exudates as germination stimulants of root parasitic plants (Cook et al., 1966; Bouwmeester et al., 39 40 2021). SLs exuded into soil promote symbiotic interactions between roots and arbuscular mycorrhizal fungi, partly by stimulating hyphal branching (Akiyama et al., 2005; Gomez-41 42 Roldan et al., 2008; Kobae et al., 2018). SLs are also plant hormones with many roles, including regulation of shoot branching, root growth, cambial growth, senescence, 43 44 defense, and anthocyanin biosynthesis (Gomez-Roldan et al., 2008; Umehara et al., 2008; Agusti et al., 2011; Rasmussen et al., 2012; Van Ha et al., 2014; Yamada et al., 45 2014; Ueda and Kusaba, 2015; Soundappan et al., 2015; Villaécija-Aguilar et al., 2019; 46 Nasir et al., 2019; Lahari et al., 2019; Kalliola et al., 2020; Wang et al., 2020a; Li et al., 47 48 2020b). KARs are abiotic signals found in smoke and biochar (Flematti et al., 2004; 49 Kochanek et al., 2016). KARs promote germination of many plant species after fire, but can also stimulate species from non-fire prone environments such as Arabidopsis thaliana 50 51 (Flematti et al., 2004; Nelson et al., 2012). In addition, KAR signaling influences seedling photomorphogenesis, mesocotyl elongation, root and root hair growth, and abiotic stress 52 53 responses (Jain et al., 2006; Nelson et al., 2010; Li et al., 2017; Wang et al., 2018; 54 Swarbreck et al., 2019; Villaécija-Aquilar et al., 2019; Li et al., 2020b; Zheng et al., 2020). 55 Despite their different sources and effects, SLs and KARs are perceived similarly 56 57 (Blázquez et al., 2020). The core SL signaling pathway in angiosperms consists of a receptor DWARF14 (D14)/DECREASED APICAL DOMINANCE2 (DAD2)/RAMOSUS3 58 59 (RMS3), an F-box protein DWARF3 (D3)/MORE AXILLARY GROWTH2 (MAX2), and transcriptional co-repressors in the SUPPRESSOR OF MAX2 1 (SMAX1)-LIKE (SMXL) 60 61 family that are known as DWARF53 (D53) in rice (Oryza sativa) or SMXL6, SMXL7, and 62 SMXL8 in Arabidopsis thaliana (Gomez-Roldan et al., 2008; Umehara et al., 2008; Waters 63 et al., 2012; Hamiaux et al., 2012; Stanga et al., 2013; Jiang et al., 2013; Zhou et al., 2013; de Saint Germain et al., 2016). D14 is an α/β -hydrolase that cleaves an enol-ether 64 65 linked methylbutenolide "D-ring" from SLs (Hamiaux et al., 2012; Seto et al., 2019). The D-ring becomes covalently attached to a His residue in the catalytic triad (Yao et al., 2016; 66

67 de Saint Germain et al., 2016). D14 changes conformation during SL binding or hydrolysis, promoting interactions with D3/MAX2 and D53/SMXL6/7/8 (Jiang et al., 2013; Zhou et al., 68 69 2013; Wang et al., 2015; Yao et al., 2016). D14 is central to formation of the tripartite complex, but D3 and D53 help stabilize it (Liang et al., 2016; Shabek et al., 2018). 70 71 D3/MAX2 functions within an SCF-type (Skp1, Cullin, F-box) E3 ubiquitin ligase complex. 72 SCF^{MAX2} polyubiquitinates D53/SMXL6/7/8 proteins, which are then rapidly degraded by 73 the 26S proteasome (Jiang et al., 2013; Zhou et al., 2013; Soundappan et al., 2015; Wang 74 et al., 2015; Yao et al., 2016; Shabek et al., 2018). D14 is also degraded after SLactivation in a MAX2-dependent manner, but this occurs over hours rather than minutes 75 76 (Chevalier et al., 2014; Hu et al., 2017).

77

KAR signaling shares a requirement for MAX2, but an ancient D14 paralog, KARRIKIN 78 79 INSENSITIVE 2 (KAI2)/HYPOSENSITIVE TO LIGHT (HTL), acts as a receptor and SMAX1 and SMXL2 are downstream targets (Sun and Ni, 2011; Nelson et al., 2011; 80 81 Waters et al., 2012; Stanga et al., 2013; Stanga et al., 2016; Khosla et al., 2020b; Zheng 82 et al., 2020). Similar to SL signaling, activation of KAI2 triggers its association with MAX2 and SMAX1/SMXL2, leading to SMAX1 and SMXL2 degradation (Yao et al., 2017; Xu et 83 84 al., 2018; Wang et al., 2020b; Khosla et al., 2020b; Zheng et al., 2020; Carbonnel et al., 2020a; Wang et al., 2021). Polyubiquitination of SMXL2 has been demonstrated, and is 85 86 presumed for SMAX1 (Wang et al., 2020b). KAI2 is also degraded after activation, although unlike D14 this is SMAX1/SMXL2-dependent rather than MAX2-dependent 87 88 (Waters et al., 2015b; Khosla et al., 2020b). In addition to mediating KAR responses, KAI2 is thought to recognize an endogenous signal, KAI2 ligand (KL), that remains 89 90 undiscovered (Conn and Nelson, 2015; Waters et al., 2015a). KAI2 is more sensitive to 91 desmethyl butenolide compounds than methylbutenolide compounds, which may give 92 hints about the chemical structure of KL (Yao et al., 2021). KARs themselves likely require 93 metabolism in plants to be recognized by KAI2 (Waters et al., 2015a; Xu et al., 2018; 94 Wang et al., 2020b; Khosla et al., 2020b; Nelson, 2021).

95

96

97

There is substantial evidence that SL and KAR/KL pathways function independently despite their homology. First, SL and KAR treatments usually affect different aspects of

98 plant growth (Waters et al., 2017). For example, SLs inhibit shoot branching, while KARs promote Arabidopsis germination (Nelson et al., 2011; Scaffidi et al., 2014). Second, genetic analysis often shows different roles for SL and KAR/KL pathway genes. SLinsensitive and SL-deficient mutants often have different phenotypes than the KAR/KLinsensitive mutant kai2 (Nelson et al., 2011; Waters et al., 2012; Villaécija-Aguilar et al., 2019). Likewise, smax1 (or smax1 smxl2) and smxl6,7,8 mutants suppress different max2 phenotypes that are associated with KAR/KL and SL insensitivity, respectively (Stanga et al., 2013; Soundappan et al., 2015; Wang et al., 2015; Stanga et al., 2016; Swarbreck et al., 2019; Villaécija-Aguilar et al., 2019). In some cases, however, such as drought resistance or mesocotyl elongation, both pathways may influence a trait (Li et al., 2020b; Zheng et al., 2020). Third, promoter-swapping experiments show that KAI2 and D14 are not interchangeable genes whose unique roles arise from different expression patterns (Waters et al., 2015a; Carbonnel et al., 2020b). Fourth, D14 and KAI2 prefer to interact with different SMXL targets (Yao et al., 2017; Wang et al., 2020b; Khosla et al., 2020b; Zheng et al., 2020). Receptor-SMXL interaction specificity is linked to the central D1M domains of SMXL proteins (Khosla et al., 2020b). Fifth, KAR treatment triggers degradation of SMAX1-type but not D53-type SMXL proteins (Jiang et al., 2013; Wang et al., 2015; Khosla et al., 2020b; Zheng et al., 2020). Transient coexpression of SL and KAR/KL signaling components from Lotus japonicus in Nicotiana benthamiana also suggest the specific degradation of SMAX1 by KAI2 and a D53-type SMXL by D14 (Carbonnel et al., 2020a). Finally, evolutionary analysis indicates that D14 was derived from KAI2 and D53-type SMXL proteins were derived from SMAX1-type SMXLs (Bythell-Douglas et al., 2017; Walker et al., 2019). Coevolution of D14 and D53-type SMXLs may have produced an orthogonal SL signaling pathway.

122

123

124

125

126

127

128

99

100

101

102

103

104

105

106

107

108

109

110

111

112

113

114

115

116

117

118

119

120

121

Recent work has challenged the model of insulated SL and KAR pathways. Genetic studies of lateral root development and root skewing initially implied that KAI2 may target SMXL6, SMXL7, and SMXL8 (Swarbreck et al., 2019). However, lateral root development was later shown to be additively regulated by SL and KAR/KL pathways, putatively with shifting contributions from each at different developmental stages (Villaécija-Aguilar et al., 2019). The effect of smxl6,7,8 on root skewing, which is KAI2-regulated, has been

inconsistent between different labs (Swarbreck et al., 2019; Villaécija-Aguilar et al., 2019). Thus, there is not strong support for KAI2-SMXL6,7,8 crosstalk. By contrast, there is compelling biochemical evidence that D14 can target SMXL2 (Wang et al., 2020b). SMXL2 co-immunoprecipitates D14 in the presence of GR24^{5DS} or GR24^{4DO}, synthetic SL analogs of the natural SLs 5-deoxystrigol (5DS) and 4-deoxyorobanchol (4DO). Furthermore, GR24^{4DO} promotes the polyubiquitination and degradation of SMXL2 through D14 in the *kai2* background (Wang et al., 2020b). This indicates that one-way crosstalk between the SL and KAR pathways is possible, while also raising the guestion of whether it occurs naturally.

Co-immunoprecipitation of D14 by SMAX1 was not observed, and it is unknown whether D14 can stimulate SMAX1 degradation (Wang et al., 2020b). However, the potential for D14-SMAX1 crosstalk has been suggested by D14-mediated effects of GR24 on hypocotyl elongation, root hair density, and root hair elongation, which are controlled by SMAX1 and SMXL2 (Waters et al., 2012; Toh et al., 2014; Stanga et al., 2016; Villaécija-Aguilar et al., 2019). We investigated whether D14 can interact with SMAX1 and target it for degradation. Here we report that *KAI2*-independent hypocotyl inhibition in the presence of a SL analog is genetically dependent on *D14* and *MAX2*, and is primarily due to destabilization of SMAX1. Although the ability of D14 to interact with SMAX1 and SMXL2 may be a little-used vestige of its evolution from KAI2, this crosstalk shows physiological relevance for osmotic stress responses in seedlings.

RESULTS

Genetic evidence for D14 crosstalk with SMAX1 and SMXL2 in seedlings

KAR₁, KAR₂, and *rac*-GR24 (a racemic mixture of GR24^{5DS} and GR24^{ent-5DS}) inhibit hypocotyl elongation of Arabidopsis seedlings grown under continuous red light (Nelson et al., 2010). GR24^{5DS} has a D-ring in the stereochemical configuration of natural SLs and signals through D14. Its enantiomer, GR24^{ent-5DS}, has a D-ring configuration that is not found in SLs. GR24^{ent-5DS} signals mostly through KAI2 but can also activate D14 *in vitro* and *in vivo* (Scaffidi et al., 2014; Waters et al., 2015a; Flematti et al., 2016). Although *kai2* seedlings are insensitive to KAR₂ and mostly insensitive to GR24^{ent-5DS}, responses to *rac*-

GR24 and GR24^{5DS} remain (Waters et al., 2012; Scaffidi et al., 2014). We first tested whether KAl2-independent responses to GR24 require MAX2. *Rac*-GR24 and GR24^{5DS} had no effect on *kai2 max2* hypocotyl, validating that responses to these compounds are *MAX2*-dependent (Supplemental Figure 1).

We next examined genetic interactions among *kai2*, *d14*, *smax1*, and *smxl* mutants to determine which *SMXL* genes are epistatic to *KAI2* and *D14* (Figure 1 and Supplemental Figure 2). As shown previously, *d14-1* had wild-type hypocotyl elongation under control conditions, implying that endogenous SLs do not affect hypocotyl growth. In contrast, *kai2* had elongated hypocotyls and *smax1 smxl2* hypocotyls were very short (Waters et al., 2012; Stanga et al., 2016). The *kai2 d14-1* double mutant was similar to *kai2*, but was also insensitive to GR24 treatments, indicating that *KAI2*-independent responses to GR24 occur through *D14* (Scaffidi et al., 2014). The *kai2 smax1 smxl2* and *d14-1 smax1 smxl2* triple mutants showed dramatically decreased hypocotyl lengths that were not further affected by KAR₂ or GR24 treatments, similar to *smax1 smxl2*. This indicated that *SMAX1* and *SMXL2* are epistatic to *KAI2* (Figure 1).

Because hypocotyl elongation of *d14* is similar to wild type, however, the *d14-1 smax1 smxl2* triple mutant did not clarify whether SMAX1 and SMXL2 also act downstream of D14 or function in a separate pathway. We found evidence for the former idea by excluding a role for *SMXL6*, *SMXL7*, and *SMXL8* in hypocotyl growth. We did not observe an appreciable difference between *smxl6*,7,8 and wild-type seedlings under control conditions or in their responses to KAR2 or GR24 (Figure 1). Moreover, *smxl6*,7,8 mutations did not substantially affect the length of *kai2* or *d14-1* hypocotyls under control conditions or their responses to KAR2 and GR24 treatments, in clear contrast to *smax1 smxl2*. Therefore, D14-mediated responses to *rac*-GR24 and GR24^{5DS} in seedling hypocotyls are not due to SMXL6,7,8 degradation. Instead, D14 is likely to target SMAX1 and/or SMXL2 for degradation in the presence of GR24.

SMAX1 is the primary regulator of hypocotyl growth targeted by KAI2 and D14

Given the biochemical evidence for D14 interactions with SMXL2 but not SMAX1, we hypothesized that D14 may target SMXL2 for degradation more effectively than SMAX1 (Wang et al., 2020b). To assess whether KAI2 and D14 differentially target SMAX1 and SMXL2 during hypocotyl elongation, we compared the growth of d14-1 smax1, d14-1 smxl2, kai2 smax1, and kai2 smxl2 seedlings (Figure 2). Consistent with the larger role of SMAX1 in hypocotyl elongation, smax1 dramatically suppressed the elongated hypocotyl phenotype of kai2, while smxl2 had little effect (Stanga et al., 2016). Responses to rac-GR24 and GR24^{5DS} were similarly strong in kai2 smxl2 and kai2, putatively reflecting the ability of D14 to act upon SMAX1 (Figure 2 and Supplemental Figure 3). Interestingly, the average hypocotyl length of seedlings treated with rac-GR24 was slightly shorter for kai2 smax1 (in which D14 and SMXL2 remain) than d14-1 smax1 (in which KAI2 and SMXL2 remain), suggesting that D14 may target SMXL2 better than KAI2. Conversely, the hypocotyl length of seedlings treated with rac-GR24 was slightly longer for kai2 smxl2 than d14-1 smxl2, suggesting that KAI2 may target SMAX1 better than D14 (Figure 2). A similar pattern of results was observed in treatments with purified GR24 stereoisomers (Supplemental Figure 3).

SMAX1 is degraded after GR24^{5DS} treatment by D14-SCF^{MAX2} signaling

We next used a ratiometric reporter system to investigate whether D14 can induce degradation of Arabidopsis SMAX1 and SMXL2 proteins (Figure 3)(Khosla et al., 2020a; Khosla et al., 2020b). We transiently expressed pRATIO1212-SMAX1, -SMXL2, and -SMAX1_{D2} (a C-terminal domain of SMAX1 sufficient for degradation, see below) dual-fluorescent reporter constructs in wild-type *N. benthamiana* leaves and tested the effects of 10 μM KAR1 and GR24^{5DS} treatments on excised leaf discs. The ratio of mScarlet-I/Venus fluorescence decreased for all constructs in response to both treatments, indicating degradation of SMAX1-, SMXL2-, and SMAX1_{D2}-mScarlet-I fusion proteins (Figure 3A-3C). The extent of degradation induced by GR24^{5DS} was similar to KAR1. Although GR24^{5DS} responses are predominantly mediated by D14 in Arabidopsis, we could not assume that GR24^{5DS}-induced degradation of SMAX1 and SMXL2 in *N. benthamiana* is due to D14 alone. Therefore we also tested these constructs in a *N. benthamiana* d14a d14b double mutant (*Nbd14*) background (White et al., 2021). The

SMXL7 reporter was unaffected by *rac*-GR24 in *Nbd14*, indicating that its degradation is specifically mediated by *N. benthamiana* D14 proteins and not KAI2 (White et al., 2021). In *Nbd14* leaves, we observed 55% and 51% less degradation of SMAX1 and SMXL2 reporters, respectively, after 12 h treatment with GR24^{5DS} compared to KAR₁ (Figure 3A and 3B). At an earlier 4 h time point, GR24^{5DS} had very little effect on SMAX1 degradation compared to KAR₁ in the *Nbd14* mutant, but was effective in wild type (Supplemental Figure 4). This indicated that *N. benthamiana* D14 proteins mediate much, although not all, of the GR24^{5DS}-induced degradation of SMAX1 and SMXL2.

To verify that D14 can cause SMAX1 degradation, we rescued the *Nbd14* mutant by transient expression of Arabidopsis *D14*. As a negative control, we tested the d14^{S97A} mutant, which has no SL hydrolysis or signaling activity (Waters et al., 2015a; Seto et al., 2019). We also tested the *seto5/d14-2* allele of Arabidopsis *D14* (here *d14^{seto}*, to avoid confusion with the *Osd14-2* allele in rice). The *d14^{seto}* mutant has increased axillary bud outgrowth, similar to the loss-of-function T-DNA insertion allele *d14-1* (Chevalier et al., 2014). Co-expression of D14 restored the degradation of SMAX1 and SMXL7 reporters following GR24^{5DS} treatment in *Nbd14* leaves (Figure 3D and 3E). By contrast, d14^{S97A} failed to restore GR24^{5DS}-induced degradation of SMAX1 and SMXL7. Interestingly, d14^{seto} enabled GR24^{5DS}-induced degradation of SMAX1 and SMXL7, similar to D14. Moreover, in the absence of GR24^{5DS} treatment, *d14^{seto}* co-expression reduced the accumulation of SMAX1 reporter relative to *D14* co-expression (Figure 3D and 3E). Therefore, the *d14^{seto}* allele does not cause a complete loss-of-function and may be more effective at triggering SMAX1 degradation.

We next investigated whether SMAX1 degradation in Arabidopsis also involves D14. We have not yet been successful in detecting full-length SMAX1 in Arabidopsis (Khosla et al., 2020b). However, the C-terminal D2 domain of SMAX1 (SMAX1_{D2}) is more stable than SMAX1, and is necessary and sufficient for MAX2-mediated degradation if full-length SMAX1 and/or SMXL2 proteins are also present. SMAX1_{D2} lacks the central D1M domains that mediate interactions between SMXL proteins and their receptor partners, KAI2 or D14, and therefore is likely to be targeted for degradation indirectly through

association with SMAX1 or SMXL2 (Khosla et al., 2020b). D14-mediated, GR24^{5DS}-induced degradation of the SMAX1_{D2} ratiometric reporter in *N. benthamiana*, was similar to full-length SMAX1 and SMXL2 reporters (Figure 3C). Therefore, we crossed *kai2* and *d14-1* mutations into a stable transgenic SMAX1_{D2}-LUC reporter line in Arabidopsis to analyze KAR₂- and GR24^{5DS}-induced degradation responses (Khosla et al., 2020b). KAR₂ caused a significant decline in SMAX1_{D2}-LUC bioluminescence within 4 h in wild-type and *d14-1* seedlings, but had no effect in *kai2* or *max2* seedlings (Figure 3F). By contrast, GR24^{5DS} caused a decline in the abundance of SMAX1_{D2}-LUC reporter in wild-type and *kai2* seedlings, but not in *d14-1* or *max2* seedlings (Figure 3G). This demonstrated that GR24^{5DS}-induced degradation of SMAX1_{D2} (and by proxy, SMAX1 and/or SMXL2) in Arabidopsis is due to D14 and MAX2 activity.

GR24^{5DS} promotes interactions of D14 with SMAX1 and SMXL2

To determine whether D14 targets SMAX1 and SMXL2 directly, we investigated interactions among these proteins. In yeast two-hybrid (Y2H) assays, GR24^{5DS} stimulated protein-protein interactions between D14 and SMAX1, SMXL2, and SMXL7. Based upon the relative growth rates of yeast under low-stringency histidine dropout selection, D14-SMAX1 interactions were weaker than D14-SMXL2 and D14-SMXL7 interactions and not very different from a GAL4 activation domain (AD) negative control. In the presence of GR24^{5DS}, D14 had stronger interactions with the D1M domains of SMAX1 and SMXL7 (SMAX1_{D1M} and SMXL7_{D1M}) than the full-length proteins, as indicated by yeast growth under higher-stringency histidine and adenine dropout selection. Again, D14 showed a stronger interaction with SMXL7_{D1M} than SMAX1_{D1M} (Figure 4A). As a negative control, we tested d14^{S97A} and observed no interactions (Supplemental Figure 5).

We also investigated SMAX1 and SMXL7 interactions with d14^{seto}, which has an amino acid substitution at the solvent-exposed surface of a D14 cap helix that might influence protein-protein interactions (Chevalier et al., 2014). We observed that d14^{seto} had highly reduced or abolished Y2H interactions with SMAX1, SMXL2, SMXL7, SMXL7_{D1M}, and the GAL4 activation domain (AD) itself in the presence of GR24^{5DS} compared to D14.

Unexpectedly, d14^{seto} maintained interactions with SMAX1_{D1M} and, furthermore, interacted with SMAX1_{D1M} in the absence of GR24^{5DS} (Figure 4A).

284

285

286

287

288

289

290

291

292

293

294

295

296

297

298

299

300

301

302

303

304

305

306

307

308

309

310

311

283

282

To validate the Y2H results in a plant system, we examined D14 interactions with SMXL proteins using split-luciferase assays in N. benthamiana leaves. N- and C-terminal portions of firefly luciferase (LUC) were fused respectively to the C-termini of SMXL proteins and the N-termini of D14, d14^{seto} or d14^{S97A}. To normalize transformation efficiencies across samples, the fluorescent protein mCherry was co-expressed with the split-luciferase constructs. These assays were performed in Nbd14 leaves to avoid possible interference from native NbD14 proteins. The ratio of LUC to mCherry signal produced by cLUC-D14 and SMXL7-nLUC was significantly higher than for unfused cLUC or nLUC negative controls. GR245DS further increased the LUC/mCherry ratio for D14-SMXL7, consistent with an enhanced protein-protein interaction. Although d14^{S97A} produced a similar interaction with SMXL7 as D14 under control conditions, GR24^{5DS} had no effect (Figure 4B). In contrast to the Y2H experiments, d14^{seto} appeared to interact with SMXL7 similarly to D14, albeit with a putatively reduced response to GR24^{5DS}. We next tested D14 interactions with SMAX1 and SMXL2. We were unable to detect LUC/mCherry signal for D14-SMAX1 above that of negative controls even in the presence of GR24^{5DS} (Supplemental Figure 6). This may be due to the instability of SMAX1 (Khosla et al., 2020b). Deletion of a conserved P-loop motif (RGKT) causes resistance to SCF^{MAX2}-mediated degradation in D53-type SMXL proteins as well as SMAX1 and SMXL2 (Jiang et al., 2013; Zhou et al., 2013; Soundappan et al., 2015; Wang et al., 2015; Liang et al., 2016; Khosla et al., 2020b; Wang et al., 2020b). Therefore, we tested interactions between SMAX1^A RGKT and D14. This enabled detection of a GR24^{5DS}responsive interaction with D14, although with a much lower signal than D14-SMXL7 or D14-SMXL2. SMAX1^A RGKT and SMXL2 interactions with D14, d14^{seto}, and d14^{S97A} were qualitatively similar to those observed for SMXL7, with a positive GR245DS response maintained for d14^{seto} but not d14^{S97A} (Figure 4C and 4D). SMAX1_{D1M} and SMXL7_{D1M} showed a similar pattern of interactions with D14 and d14 mutant proteins as full-length SMXL proteins, but produced stronger luminescence signals (Figure 4E and 4F,

Supplemental Figure 7). In contrast to the Y2H experiments, we did not observe reduced interactions between SMXL7_{D1M} and d14^{seto} compared to D14.

314

315

316

317

318

319

320

321

322

323

324

325

326

327

328

329

330

331

332

333

334

335

312

313

The differing results from Y2H and split-LUC assays led us to further examine D14 and d14^{seto} interactions with SMAX1 and SMXL7 by measuring Förster resonance energy transfer after acceptor photobleaching (FRET-APB) (Day et al., 2001). This technique determines FRET efficiency, which is a measure of protein-protein interactions, by comparing the fluorescence of the donor (e.g. GFP) before and after photobleaching of the acceptor (e.g. mCherry). We performed FRET-APB assays with D14-GFP, d14^{seto}-GFP, and SMAX1-mCherry fusion proteins coexpressed in N. benthamiana leaves. Photobleaching of SMAX1-mCherry caused a negligible change in fluorescence of a myc-GFP negative control, indicating an absence of FRET between these two proteins (Figure 4G). By contrast, FRET was detected between D14-GFP and SMAX1-mCherry. After 5 min of treatment with a solvent control, SMAX1-mCherry photobleaching caused a small rise in D14-GFP fluorescence. Treatment with GR24^{5DS} for 5 min or 30 min increased the FRET efficiency approximately two- to three-fold above the solvent control. Similar results were obtained for d14^{seto}-GFP and SMAX1-mCherry. The average FRET efficiency between d14seto-GFP and SMAX1-mCherry was higher than for D14-GFP and SMAX1mCherry after 30 min of GR24^{5DS} treatment (10.4% versus 6.9%, respectively), although this difference was not statistically significant (p = 0.24, Student's t-test). We also examined D14-SMXL7 interactions with FRET-APB. The FRET efficiency between D14 and SMXL7 peaked within 5 min of GR24^{5DS} treatment. Similar FRET efficiencies in the presence and absence of GR24^{5DS} were observed between d14^{seto} and SMXL7 (Figure 4H).

336

337

338

339

340

341

342

Altogether, these experiments indicate that D14 and SMAX1 can associate in the presence of GR24^{5DS}. Y2H and split-LUC experiments suggest that D14 can interact better with SMXL2 than SMAX1, although this may be due, at least in part, to the instability of SMAX1 (Figure 4 and Supplemental Figure 7). The effect of d14^{seto} is less clear. Although Y2H experiments suggested that d14^{seto} is less able to interact with SMAX1, SMXL2, and SMXL7, this was not supported by split-LUC and FRET-APB assays in

plants. The differences could be a consequence of overexpression or the effects of other proteins in the plant cell environment (e.g. MAX2) on D14 signaling, interactions, and stability. Regardless, d14^{seto} was not as deficient in its interactions with SMXL proteins or GR24^{5DS} response as d14^{S97A}, suggesting it is hypomorphic rather than amorphic.

A hypomorphic d14 protein is more active when SMAX1 and SMXL2 are absent Although D14 can induce degradation of SMAX1 and SMXL2, it was unclear whether this is only an artifact of treatments with an exogenous SL analog. If D14-mediated degradation of SMAX1 and SMXL2 has physiological significance, we can expect *d14* to affect growth processes controlled by SMAX1 and SMXL2 and/or *smax1 smxl2* to at least partially suppress *d14* phenotypes. As noted above, *d14-1* seedlings are phenotypically similar to the wild type. We found that *d14seto* hypocotyls were slightly shorter than the wild type, suggesting SMAX1/SMXL2 might be partially reduced (Supplemental Figure 8). However, *d14seto* and *kai2 d14seto* showed little response to GR24^{5DS}, implying any such targeting by d14seto might reflect promiscuous activity rather than a SL response, as suggested by Y2H (Figure 4A and Supplemental Figure 8).

We next examined the effects of *KAI2*, *SMAX1*, and *SMXL2* on the excess shoot branching phenotype of *d14*. A recent study based on overexpression of *SMAX1* proposed that SMAX1 suppresses axillary shoot branching (Zheng et al., 2021). Countering this, we did not observe any effect of *kai2*, which overaccumulates SMAX1 and SMXL2, or *smax1 smxl2* on the excess branching phenotype of *d14-1* (Figure 5A and 5B). We also investigated genetic interactions between *d14seto* and KAR signaling mutants. The excess branching phenotype of *d14seto* was weaker than *d14-1*, consistent with d14seto causing a partial loss of function. Interestingly, branching number was increased to *d14-1* and *max2* levels in the *kai2 d14seto* mutant, and reduced in *d14seto smax1 smxl2*. Because *max2* was epistatic in the *d14seto smax1 smxl2 max2* mutant, SMAX1 and SMXL2 are unlikely to regulate shoot branching downstream of MAX2. Instead, these data suggest that SMAX1 and SMXL2 negatively impact the ability of d14seto to target SMXL6, SMXL7, and SMXL8 for degradation.

We found further support for this idea from analysis of *BRANCHED1* (*BRC1*) expression in non-elongated axillary buds. BRC1 is a transcription factor that represses axillary bud outgrowth whose expression is negatively regulated by SMXL6, SMXL7, and SMXL8 (Aguilar-Martínez et al., 2007; Soundappan et al., 2015; Wang et al., 2020a). Consistent with the shoot branching data, *smax1 smxl2* did not increase *BRC1* expression in the *d14-1* background. *BRC1* expression was higher in *d14seto* buds than *d14-1*, and the addition of *smax1 smxl2* mutations further increased *BRC1* expression in a *MAX2*-dependent manner (Figure 5C).

SMAX1 and SMXL2 may enhance D14 turnover after strigolactone perception

One way that SMAX1 and SMXL2 might affect the activity of d14^{seto} is by reducing its abundance. D14 and KAI2 are both degraded within hours after activation (Chevalier et al., 2014; Waters et al., 2015b; Hu et al., 2017). KAI2 degradation after KAR treatment is MAX2-independent, and likely occurs through association with SMAX1 and SMXL2, which are unstable (Waters et al., 2015b; Khosla et al., 2020b). D14 degradation after GR24 treatment is MAX2-dependent in Arabidopsis (Chevalier et al., 2014). If d14^{seto} is more prone to interactions with SMAX1 (Figure 4A and 4C), however, it might undergo increased turnover compared to wild-type D14. This led us to test the degradation of D14-GFP and d14^{seto}-GFP fusions expressed in wild-type seedlings following treatment with *rac*-GR24. We observed a faster rate of decline for d14^{seto}-GFP than D14-GFP in both hypocotyl and root tissues of seedlings after *rac*-GR24 treatment (Figure 6A).

To assess whether SMAX1 and SMXL2 influence GR24^{5DS}-induced degradation of D14, we next introduced a *UBQ:D14-LUC* transgene into wild-type and *smax1 smxl2* backgrounds. The decline in bioluminescence from D14-LUC following GR24^{5DS} treatment was slowed in *smax1 smxl2* at all time points in comparison with wild-type, suggesting that D14-LUC was partially stabilized by the absence of SMAX1 and SMXL2 (Figure 6B). We then transiently expressed *D14*, *d14*^{seto}, and *d14*^{S97A} ratiometric reporters with or without Arabidopsis SMAX1 in *Nbd14* leaves (Figure 6C). The d14^{S97A} reporter was the most stable of the three variants; it showed the highest relative abundance and was unaffected by GR24^{5DS} treatment. D14 and d14^{seto} reporters both declined during the

12 hours following GR24^{5DS} treatment. As in Arabidopsis, d14^{seto} showed a faster rate of decline. Coexpression of *SMAX1* caused a small, but significant, increase in GR24^{5DS}-induced turnover of D14 at two time points and of d14^{seto} at all time points. This suggested that D14 interaction with SMAX1 and SMXL2 may reduce its abundance in the presence of GR24; increased availability of a partially active d14^{seto} protein might explain why the *d14^{seto} smax1 smxl2* mutant showed partially recovered shoot branching.

D14-SCF^{MAX2} mediates SMAX1 degradation induced by osmotic stress

Although D14 and KAI2 often affect different developmental traits, this is not always the case. For example, both SL and KAR/KL pathways promote drought tolerance in Arabidopsis (Li et al., 2017; Haider et al., 2018; Li et al., 2020a; Li et al., 2020b). Our data suggested that D14 has no effect on SMAX1 and SMXL2 degradation in response to endogenous SLs during seedling photomorphogenesis or shoot branching. We reasoned that D14-mediated degradation of SMAX1 and SMXL2 might be physiologically relevant for some traits regulated by both pathways, or under conditions in which endogenous SL levels are sufficiently high. SL biosynthesis genes are induced by dehydration or mild drought in Arabidopsis and rice, leading to increased SL in rice roots at least (Van Ha et al., 2014; Haider et al., 2018).

Therefore, as an alternative form of imposing drought/water-deficit, we examined the response of KAR and SL signaling pathway mutants to osmotic stress. Wild-type seedlings grown in the presence of 300 mM mannitol showed a 40% reduction in fresh weight compared to those grown on standard medium (Figure 7A and 7B). Growth inhibition by mannitol was enhanced in *d14* and *kai2* seedlings and mannitol also caused a reduction in chlorophyll content (Figure 7A and 7C). We found that *smxl6*, 7,8 seedlings were even more strongly affected by mannitol than *kai2* and *d14*. By contrast, *smax1 smxl2* seedlings were resistant to mannitol, showing only a 10% reduction in fresh weight and an increase in chlorophyll content under mannitol treatment. Intriguingly, *SMAX1* and *SMXL2* contributed differently to osmotic stress tolerance. Under mannitol treatment we observed less reduction in biomass in *smax1* seedlings and higher chlorophyll content in *smxl2* seedlings compared to wild-type (Supplemental figure 9).

To assess the effect of *smax1 smxl2* or *smxl6*,7,8 mutant on osmotic stress-induced gene expression, we performed quantitative RT-PCR of *RD29A*, *Cor15A* and *PKS5* (Fujii et al., 2011; Liu et al., 2014). Induction of *RD29A*, *Cor15A*, and *PKS5* transcripts in response to mannitol treatment was impaired in *smax1 smxl2* seedlings. In comparison, *RD29A* showed normal upregulation in response to mannitol treatment in *smxl6*,7,8 seedlings. *Cor15A* and *PKS5* were not as highly induced by mannitol in *smxl6*,7,8 seedlings than wild-type, but were more highly induced than in *smax1 smxl2* (Figure 7E).

Because *smax1 smxl2* had opposite phenotypes to *d14* as well as *kai2*, and was epistatic to both, we hypothesized that D14 may contribute to SMAX1 and SMXL2 degradation during mannitol treatment. To test this, we compared degradation of the SMAX1_{D2}-LUC reporter after mannitol treatment in Col-0, *kai2*, *d14-1*, *max2*, and the SL biosynthetic mutant *max3*. We observed degradation of SMAX1_{D2}-LUC within 8 h of mannitol treatment in wild-type and *kai2* seedlings, but not in *d14-1*, *max2*, or SL-deficient *max3* seedlings (Figure 7D). SMXL7-LUC was also destabilized in a *D14*-dependent manner under mannitol treatment, supporting the idea that the level of endogenous SL and/or D14-SCF^{MAX2} signaling is induced by osmotic stress (Supplemental figure 10). These results suggest that SL-induced degradation of SMAX1 and SMXL2 via D14-SCF^{MAX2} is not just an artificial consequence of GR24 application, but can also occur under specific environmental conditions.

DISCUSSION

Despite KAR/KL and SL signaling pathways having strong similarities, genetic and biochemical studies have suggested that they are well-insulated by specific receptor-target interactions, enabling distinct developmental responses to KAR/KL and SL (Soundappan et al., 2015; Villaécija-Aguilar et al., 2019). Contradicting this model, here we have shown that D14 can target SMAX1 for degradation after SL analog treatments. Genetic tests indicated that SMAX1 and, to a lesser degree, SMXL2 regulate hypocotyl elongation, but SMXL6, SMXL7, and SMXL8 do not (Figure 1 and 2). This implied that the D14-mediated effect of GR24 on hypocotyl elongation is due to D14-SMAX1

crosstalk. This idea was supported by the observation that a SMAX1 ratiometric reporter was degraded in *N. benthamiana* after GR24^{5DS} treatment in a partially D14-dependent manner (Figure 3A). GR24^{5DS}-induced degradation of a SMAX1_{D2} reporter in *Arabidopsis thaliana* was also blocked in the *d14* background (Figure 3G). Physical interactions between D14 and SMAX1, however, are weak at best (Figure 4). SMXL proteins, which are distantly related to HSP101 heat-shock proteins that form hexamers, may form multimeric complexes (Khosla et al., 2020b). If heterogeneous complexes form (e.g. composed of SMAX1 and non-SMAX1 subunits), it is possible that SMAX1 could be indirectly targeted for proteolysis by a non-cognate receptor (i.e. D14) that interacts with SMXL2 or SMXL7. However, SMAX1 degradation by D14 does not require the presence of SMXL2, as demonstrated by the GR24 response of *kai2 smxl2* seedlings (Figure 2). Nor does GR24-induced degradation of SMAX1 and SMXL2 by D14 require SMXL6, SMXL7, or SMXL8, as shown by *kai2 smxl6*, 7,8 seedlings (Figure 1C).

Therefore, our data suggest that a direct interaction between D14-SCF^{MAX2} and SMAX1 can occur when a SL analog is applied. Similarly, D14 can crosstalk with SMXL2 in the presence of SL analogs (Wang et al., 2020b). By contrast, there is no indication that KAR application can cause KAI2-SCF^{MAX2} to target D53 or SMXL7 for degradation, and the current genetic evidence for such crosstalk is controversial (Jiang et al., 2013; Wang et al., 2015; Swarbreck et al., 2019; Villaécija-Aguilar et al., 2019; Khosla et al., 2020b). We propose an update of the fully insulated KAR/KL and SL signaling models to include one-way promiscuity, in which D14 crosstalk with SMAX1 and SMXL2 is a putative remnant of its evolution from a KAI2 paralog (see below; Figure 8).

SMAX1 can be targeted by D14 in Arabidopsis, but less well than SMXL2

It is likely that D14 has lower affinity for SMAX1 than SMXL2. Although both SMAX1 and SMXL2 are able to co-immunoprecipitate KAI2 from Arabidopsis protoplasts in the presence of an agonist, only SMXL2 is effective at co-immunoprecipitation of D14 (Wang et al., 2020b). SMAX1 did not interact with D14 *in vitro* in a pull-down assay (Yao et al., 2017). Likewise, we observed weaker yeast two-hybrid interactions between D14 and SMAX1 than SMXL2 (Figure 4A). In addition, we saw negligible luminescence in split-

luciferase assays for D14-SMAX1 interactions compared to D14-SMXL2 or D14-SMXL7. This may be due to MAX2-dependent and/or -independent degradation of SMAX1 that causes high turnover (Khosla et al., 2020b). The luminescence signal was increased in split-luciferase assays between D14 and a degradation-resistant SMAX1^{ΔRGKT} mutant protein, although it was still weaker than that produced by D14-SMXL2 interactions (Figure 4 and Supplemental Figure 6). Finally, we note that while we observed a strong effect of 500 nM GR24^{5DS} on hypocotyl elongation of both *smax1* and *smxl2*, Wang et al. (2020) observed different D14-mediated responses to 100 nM GR24^{4DO} treatments in these mutants (Figure 2 and Supplemental Figure 3). The 100 nM GR24^{4DO} treatment had only a small effect on hypocotyl elongation of smxl2 but had a large effect on smax1 seedlings, implying that SMAX1 is less effectively degraded than SMXL2. Lower concentrations of SL may be required to induce D14 crosstalk with SMXL2 than SMAX1. For developmental processes such as root hair elongation, in which SMXL2 has a more prominent role than SMAX1, or root skewing, to which SMXL2 and SMAX1 contribute non-redundantly, it may be more likely for endogenous SLs to have an effect via D14mediated crosstalk (Villaécija-Aguilar et al., 2019). It is currently unknown whether D14 can crosstalk with SMAX1 orthologs in other species. OsSMAX1 in rice (LOC Os08g15230), at least, does not appear to be an interaction partner or target of D14 (Zheng et al., 2020).

517518

519

520

521

522

523

524

525

526

527

528

498

499

500

501

502

503

504

505

506

507

508

509

510

511

512

513

514

515

516

Evolution of target preferences in KAR/KL and SL signaling pathways

Regardless of whether non-cognate interactions between D14 and SMAX1/SMXL2 affect development under physiological conditions, it is clear that the cognate interactions between D14 and D53-type SMXL proteins are important for SL-regulated growth in plants. This raises the question of how D14 and D53-type SMXL proteins evolved specificity in their interactions that largely prevents crosstalk between the homologous SL and KAR/KL pathways in angiosperms. SLs have ancient origins in the land plant lineage (Yoneyama et al., 2018; Walker et al., 2019). However, D14 orthologs are only observed in the seed-bearing lineage (gymnosperms and angiosperms) (Bythell-Douglas et al., 2017). Gymnosperms have putative SMAX1 orthologs, but D53 orthologs are only found in angiosperms (Walker et al., 2019). Thus, the canonical D14-SCF^{MAX2}-D53 SL signaling

mechanism is a feature of angiosperms. An attractive hypothesis, however, is that KAI2-like proteins function as SL receptors that target SMAX1 for degradation in other land plants. This is quite plausible given that such a mechanism is used by the seeds of obligate parasitic plants in the Orobanchaceae to sense host-derived SLs and germinate (Nelson, 2021).

One way that selective protein-protein interactions between KAI2-SMAX1 and D14-SMXL7 could have evolved is via a mutation(s) in a SL-responsive KAI2 paralog (a proto-D14) that disrupts SMAX1 interactions combined with a compensatory mutation(s) in a SMAX1 paralog (a proto-SMXL7) that establishes an orthogonal interaction with the proto-D14. However, this evolutionary path involves an intermediate phase during which the proto-D14 is a pseudogene and/or the proto-SMXL7 is misregulated with potentially detrimental effects. Bacterial toxin-antitoxin systems have revealed an alternative way that duplicated protein pairs may evolve selective interactions: via a promiscuous intermediate state (Aakre et al., 2015). According to a promiscuity-based model, proto-D14 might first acquire a mutation that broadens its potential interaction specificity. This would enable proto-SMXL7 to acquire a mutation that blocks interaction with KAI2 but maintains interaction with proto-D14, without negatively affecting fitness. Subsequently, proto-D14 may acquire another mutation that narrows its interaction specificity to proto-SMXL7 alone. Throughout this process, SMXL7 regulation would continue. Substantial work will be needed to evaluate this hypothesis. However, we propose that the ability of D14 to engage in a non-preferred interaction with SMAX1 could be a remnant of such an evolutionary process.

Effects of the d14^{seto} allele

The d14^{seto} allele, which causes a Pro169Leu substitution, appears to reduce the selectivity of D14 against SMAX1 interaction (Figure 4A and 4C). Pro169 is a highly conserved (>90%) surface residue found within a small motif that distinguishes D14 and KAI2 proteins (ADV—P versus GDMDS, respectively) (Chevalier et al., 2014; Bythell-Douglas et al., 2017). As such, it has been hypothesized to be a specificity-determining position (Chevalier et al., 2014). Alternatively, this motif may influence SL perception. The

motif containing Pro169 composes most of a short loop that joins the aT2 and aT3 helices (also known as aE and aF) of D14. The composition of this loop affects the rigidity of the ligand-binding pocket, which in turn affects ligand affinities (Bürger et al., 2019).

Our results suggest that *d14*^{seto} causes a partial loss-of-function in SL signaling, as it had weaker branching and leaf morphology phenotypes than the null T-DNA insertion allele, *d14-1* (Figure 5B and Supplemental Figure 9). This implied that d14^{seto} was less effective at triggering SL-induced degradation of SMXL6, SMXL7, and SMXL8. However, in transient expression experiments in *N. benthamiana*, d14^{seto} showed a similar ability to interact with SMXL7 and cause its degradation as wild-type D14 (Figure 3E; 4B, 4F and 4H). Therefore, we hypothesized that d14^{seto} protein may have reduced function due to higher instability. Supporting this, we found that d14^{seto} was more rapidly degraded following GR24^{5DS} treatment than wild-type D14 in Arabidopsis and *N. benthamiana* (Figure 6A and 6C).

KAI2 degradation after KAR treatment is MAX2-independent and is likely driven by association with unstable SMAX1 and/or SMXL2 proteins (Waters et al., 2015b; Khosla et al., 2020b). We found that D14 instability was reduced in the smax1 smxl2 background (Figure 6B), suggesting that it may also be degraded by association with SMAX1 and/or SMXL2. This led us to hypothesize that enhanced d14^{seto} turnover after SL perception might be caused by stronger association with SMAX1 and/or SMXL2 compared with wildtype D14. Indeed, coexpression of SMAX1 slightly enhanced d14^{seto} degradation in N. benthamiana (Figure 6C). This hypothesis also predicts that the phenotypes of d14seto will be affected by SMAX1/SMXL2 abundance. Consistent with this, the branching phenotype of *d14*^{seto} was increased by the addition of *kai2*. Overaccumulation of SMAX1 and SMXL2 in *kai2* might further reduce d14^{seto} abundance (Figure 5B). Conversely, the excess branching of d14^{seto} was partially suppressed by smax1 smxl2, which might indicate that d14^{seto} protein has been stabilized. Similarly, *smax1 smxl2* partially suppressed the reduced BRC1 expression in d14seto seedlings (Figure 5B and 5C). By comparison, smax1 smxl2 had no effect on branching or BRC1 expression in the null d14-1 background (Figure 5B and 5C).

The physiological relevance of D14-SMAX1 crosstalk

591

592

593

594

595

596

597

598

599

600

601

602

603

604

605

606

607

608

609

610

611

612

613

614

615

616

617

618

619

620

621

Although D14 can target SMAX1 and SMXL2 for degradation after SL treatment, SLdeficient and -insensitive mutants do not show phenotypes associated with SMAX1 and SMXL2 overaccumulation, suggesting that this crosstalk does not normally occur (Nelson et al., 2011; Waters et al., 2012; Soundappan et al., 2015). Alternatively, SL levels that are sufficiently high to stimulate D14 crosstalk may only occur in limited developmental contexts. SL biosynthesis is induced by various stresses such as drought and phosphate starvation (López-Ráez et al., 2008; Van Ha et al., 2014; Haider et al., 2018). This led us to explore whether D14-SMAX1 crosstalk occurs during water stress. Interestingly, although smxl6,7,8 plants have enhanced resistance to water-deficit, opposite to d14 and SL-deficient mutants, we found that *smxl6*,7,8 seedlings are more susceptible to osmotic stress (Van Ha et al., 2014; Li et al., 2020a; Li et al., 2020b) (Figure 7A-7C). This was particularly surprising because d14 was also more susceptible to osmotic stress than the wild type. In contrast, smax1 smxl2 had enhanced resistance to osmotic stress and was epistatic to d14 and kai2 for this trait (Figure 7A-7C). Defective induction of RD29A and Cor15A expression in smax1 smx/2 may confer osmotic stress tolerance by strengthening photosynthesis and seedling growth (Msanne et al. 2011; Liu et al., 2014). Alternatively, given that *smax1 smxl2* seedlings showed better growth under mannitol treatment than wild-type, the reduced upregulation of RD29A, Cor15A, and PKS5 by mannitol may indicate that smax1 smx/2 is less susceptible to osmotic stress. Although we cannot yet explain smxl6,7,8 phenotypes, this suggested that D14 might target SMAX1 and SMXL2 under osmotic stress. Indeed, we observed enhanced degradation of a SMAX1_{D2} reporter following osmotic stress - without GR24 treatments - that was dependent on D14 and the SL biosynthesis gene MAX3. It is also notable that karrikin responsive genes are upregulated under osmotic stress (Shah et al., 2020). This implies a reduction in SMAX1 and SMXL2 levels, which could potentially be due to SL signaling activity. In conclusion, we propose that under some environmental conditions or developmental contexts D14 crosstalk initiated by SLs may broaden the ability of plants to fine-tune SMAX1 and SMXL2 regulation.

622 **ACKNOWLEDGMENTS**

- We gratefully acknowledge funding support from the US National Science Foundation
- 624 (NSF) grants IOS-1737153, IOS-1740560, and IOS-1856741 to DCN and BIO2014-
- 57011-R, BIO2017-84363-R, and FEDER funds to PC. We thank Dr. Gavin Flematti and
- 626 Dr. Adrian Scaffidi (University of Western Australia) for supplying *rac*-GR24 and purified
- 627 GR24 enantiomers.

628

629

AUTHOR CONTRIBUTIONS

- Experiments were designed, carried out, and analyzed by QL, ESM-F, AK, AW and SC.
- 631 Figure preparation by QL. Manuscript preparation by QL and DCN with contributions and
- final approval from all authors. Project design by QL, ESM-F, PC, and DCN. Funding to
- support the project was secured by PC and DCN.

634

635

CONFLICT OF INTEREST STATEMENT

The authors have no conflicts of interest to declare.

637

638

METHODS

- 639 Plant materials
- The Arabidopsis thaliana mutants d14-1, d14seto, htl-3 (a kai2 allele), d14-1 htl-3, max2-
- 641 1, smax1-2, smxl2-1, smax1-2 smxl2-1, smxl6-4 smxl7-3 smxl8-1 and max3-11 have
- been described previously (Waters et al., 2012; Stanga et al., 2013; Chevalier et al., 2014;
- Toh et al., 2014; Soundappan et al., 2015; Stanga et al., 2016). All lines are in the Col-0
- 644 ecotype. Genotyping primers are listed in Supplementary Table 1. Detailed methods are
- 645 found in Supplemental Information text.

646

647

SUPPLEMENTAL INFORMATION

- 648 Supplemental Figure 1. Hypocotyl elongation of kai2 is inhibited by rac-GR24 and
- 649 **GR24**^{5DS} through *MAX2*.
- 650 Hypocotyl length of 5-d-old seedlings of Col-0, kai2, and kai2 max2 are grown under
- continuous red light for 4 d on the 0.5x MS agar media containing 1 µM KAR₂, 1 µM rac-
- GR24, 0.5 μ M GR24^{5DS}, 0.5 μ M GR24^{ent-5DS} or acetone. Bar = 5 mm. Box-and-whisker

plots with the same letter are not significantly different from one another (Tukey HSD, p < 0.05, n ≥ 30).

655656

657

- Supplemental Figure 2. Hypocotyl growth of plant materials in Figure 1 with GR24^{5DS} or GR24^{ent-5DS} treatment.
- 658 Hypocotyl length of 5-d-old seedlings of Col-0, *kai2*, *d14-1*, *kai2 d14-1*, *smax1 smxl2*, *kai2*
- 659 smax1 smxl2, d14-1 smax1 smxl2, smxl6,7,8, kai2 smxl6,7,8 and d14-1 smxl6,7,8 are
- grown under continuous red light for 4 d on the 0.5x MS agar media containing 0.5 µM
- 661 GR24^{5DS}, 0.5 µM GR24^{ent-5DS} or acetone. Mock-treated seedling data are duplicated in
- Figure 1, which shows additional data from this experiment. Bar = 5 mm. Box-and-whisker
- plots with the same letter are not significantly different from one another (Tukey HSD, p
- 664 < 0.05, $n \ge 30$).

665 666

- Supplemental Figure 3. Hypocotyl growth of plant materials in Figure 2 with
- 667 **GR24**^{5DS} or **GR24**^{ent-5DS} treatment.
- 5-d-old seedlings of Col-0, kai2, d14-1, smax1, smxl2, kai2 smax1, d14-1 smax1, kai2
- 669 smxl2, d14-1 smxl2 are grown under continuous red light for 4 d on the 0.5x MS media
- 670 containing 0.5 μM GR24^{5DS}, 0.5 μM GR24^{ent-5DS} or acetone. Mock-treated seedling data
- are duplicated in Figure 2, which shows additional data from this experiment. Box-and-
- whisker plots with the same letter are not significantly different from one another (Tukey
- 673 HSD, p < 0.05, n \geq 30).

- 675 Supplemental Figure 4. Degradation of SMAX1, SMXL2 or SMAX1_{D2} after 4 h
- 676 treatment of KAR₁ or GR24^{5DS}.
- Relative fluorescence from the SMAX1-mScarlet-I reporter (A) or SMXL2-mScarlet-I
- reporter **(B)** or SMAX1_{D2}-mScarlet-I reporter **(C)** and the Venus reference after transient
- expression of the ratiometric system in wt tobacco and *Nbd14* is shown. Leaf discs are
- treated with acetone, 10 μ M KAR₁ ,or 10 μ M GR24^{5DS} for 4 h. Mock-treated seedling data
- are duplicated in Figure 3A to 3C, which show additional data from this experiment. n =
- 5-8 leaf discs. ns indicates no significance. *p < 0.05, **p < 0.01, Student's t-test
- comparisons to the relative fluorescence at 0 h or between compared pairs.

684 Supplemental Figure 5. Yeast two-hybrid assays for d14^{S97A} interactions with 685 686 SMAX1, SMXL2, SMXL7, SMAX1_{D1M} and SMXL7_{D1M}. The d14^{S97A} is fused to GAL4-BD. SMAX1, SMXL7 and their D1M domains are fused to 687 688 GAL4-AD. Serial 10-fold dilutions of yeast cultures are spotted onto selective growth medium (-L, -Leu; -T, -Trp; -H, -His; -A, -Ade) that is supplemented with 2 µM GR24^{5DS} 689 690 or acetone. 691 692 Supplemental Figure 6. D14, d14^{seto} and d14^{S97A} interactions with SMAX1 in split-693 luciferase assay. 694 N. benthamiana leaves are transiently co-transformed with Agrobacterium tumefaciens strains carrying cLUC, nLUC, or indicated fusions as well as a strain carrying an mCherry 695 696 transgene as a transformation control. Luminescence is measured before and 1 hour after treatment with 10 µM GR24^{5DS} and normalized against mCherry fluorescence. Box-and-697 whisker plots with the same letter are not significantly different from one another 698 699 (Student's t, p < 0.05, n = 8 leaf discs). 700 Supplemental Figure 7. Baseline of D14 interactions with SMAX1, SMXL2, SMXL7, 701 702 SMAX1_{D1M} and SMXL7_{D1M} in split-luciferase assay. 703 N. benthamiana leaves are transiently co-transformed with Agrobacterium tumefaciens 704 strains carrying cLUC, nLUC, or indicated fusions as well as a strain carrying an mCherry transgene as a transformation control. Luminescence is measured before 10 µM GR24^{5DS} 705 706 treatment, and normalized against mCherry fluorescence. n = 7-15 leaf discs. The data 707 are duplicated in Figure 4B to 4F, which show additional data from this experiment. 708 709 Supplemental Figure 8. Hypocotyl growth of Col-0 (wild type), kai2, d14seto, kai2 d14^{seto}, smax1 smxl2, d14^{seto} smax1 smxl2, max2, d14^{seto} smax1 smxl2 max2 under 710

Plants are grown under continuous red light for 4 d on the 0.5x MS agar media containing 1 μ M KAR₂, 1 μ M rac-GR24, 0.5 μ M GR24^{5DS}, 0.5 μ M GR24^{ent-5DS} or acetone. Bar = 5

711

712

713

different treatments.

- 714 mm. Box-and-whisker plots with the same letter are not significantly different from one
- 715 another (Tukey HSD, p < 0.05, n \geq 30).

716

- 717 Supplemental Figure 9. Osmotic stress tolerance of Col-0, smax1, smxl2 and smax1
- 718 **smxl2**.
- 719 (A) 21-day-old seedlings of Col-0, smax1, smxl2 and smax1 smxl2 grown in mock or
- 720 300 mM mannitol condition for 14 days. Bar = 1 cm.
- 721 **(B)** Relative fresh weights of plant materials used in **(A)** to application of 300 mM mannitol.
- The weights of aerial parts from plants grown on 0.5x MS agar medium containing 300
- 723 mM mannitol are scaled to that from plants grown on 0.5x MS agar medium. Scatter dot
- 724 plots with the same letter are not significantly different from one another (bar indicates
- 725 mean; n = 4; Student's t-test, p < 0.05).
- 726 (C) Chlorophyll (Chl) contents in the aerial parts of Arabidopsis seedlings used in (A).
- 727 Others are as in (B).

728

- 729 Supplemental Figure 10. Osmotic stress triggers SMXL7 degradation.
- 730 Bioluminescence of SMXL7-LUC in Col-0 and d14-1 backgrounds. Seedlings were
- 731 treated with 300 mM mannitol or water control. Bioluminescence is shown as relative LUC
- 732 activity and is monitored for 6 h after treatment. n = 12 seedlings. ns indicates no
- respectively. 733 significance. *p < 0.05, **p < 0.01, Student's t-test comparisons to Col-0 control at each
- time point.

735

- 736 Supplemental Figure 11. Rosette phenotypes of plant materials in Figure 5A.
- 737 Col-0 (wild type), d14-1, kai2 d14-1, d14-1 smax1, d14-1 smax1 smxl2, d14^{seto}, kai2
- 738 d14^{seto}, d14^{seto} smax1, d14^{seto} smax1 smxl2, d14^{seto} smax1 smxl2 max2 and max2 are
- 739 grown for 4 weeks under a long-day photoperiod (16 h light/8 h dark) before imaging. Bar
- 740 = 5 cm.

741

742 Supplemental Table 1. Primers used in this study.

743 **REFERENCES**

- Aakre, C. D., Herrou, J., Phung, T. N., Perchuk, B. S., Crosson, S., and Laub, M. T.
- 745 (2015). Evolving new protein-protein interaction specificity through promiscuous
- 746 intermediates. *Cell* **163**:594–606.
- 747 Aguilar-Martínez, J. A., Poza-Carrión, C., and Cubas, P. (2007). Arabidopsis
- BRANCHED1 acts as an integrator of branching signals within axillary buds. *Plant*
- 749 *Cell* **19**:458–472.
- 750 Agusti, J., Herold, S., Schwarz, M., Sanchez, P., Ljung, K., Dun, E. A., Brewer, P.
- 751 B., Beveridge, C. A., Sieberer, T., Sehr, E. M., et al. (2011). Strigolactone
- signaling is required for auxin-dependent stimulation of secondary growth in plants.
- 753 *Proc. Natl. Acad. Sci. U. S. A.* **108**:20242–20247.
- Akiyama, K., Matsuzaki, K.-I., and Hayashi, H. (2005). Plant sesquiterpenes induce hyphal branching in arbuscular mycorrhizal fungi. *Nature* **435**:824–827.
- Blázquez, M. A., Nelson, D. C., and Weijers, D. (2020). Evolution of Plant Hormone Response Pathways. *Annu. Rev. Plant Biol.* **71**:327–353.
- 758 Bouwmeester, H., Li, C., Thiombiano, B., Rahimi, M., and Dong, L. (2021).
- Adaptation of the parasitic plant lifecycle: germination is controlled by essential host signaling molecules. *Plant Physiol.* **185**:1292–1308.
- Bürger, M., Mashiguchi, K., Lee, H. J., Nakano, M., Takemoto, K., Seto, Y.,
- Yamaguchi, S., and Chory, J. (2019). Structural Basis of Karrikin and Non-natural
- Strigolactone Perception in Physcomitrella patens. *Cell Rep.* **26**:855–865.e5.
- Bythell-Douglas, R., Rothfels, C. J., Stevenson, D. W. D., Graham, S. W., Wong, G.
- 765 K.-S., Nelson, D. C., and Bennett, T. (2017). Evolution of strigolactone receptors
- by gradual neo-functionalization of KAI2 paralogues. *BMC Biol.* **15**:52.
- 767 Carbonnel, S., Das, D., Varshney, K., Kolodziej, M. C., Villaécija-Aguilar, J. A., and
- **Gutjahr, C.** (2020a). The karrikin signaling regulator SMAX1 controls Lotus
- japonicus root and root hair development by suppressing ethylene biosynthesis.
- 770 *Proc. Natl. Acad. Sci. U. S. A.* **117**:21757–21765.
- 771 Carbonnel, S., Torabi, S., Griesmann, M., Bleek, E., Tang, Y., Buchka, S., Basso,
- 772 V., Shindo, M., Boyer, F.-D., Wang, T. L., et al. (2020b). Lotus japonicus karrikin
- receptors display divergent ligand-binding specificities and organ-dependent
- 774 redundancy. *PLoS Genet.* **16**:e1009249.
- 775 Chevalier, F., Nieminen, K., Sánchez-Ferrero, J. C., Rodríguez, M. L., Chagoyen,
- 776 M., Hardtke, C. S., and Cubas, P. (2014). Strigolactone promotes degradation of
- DWARF14, an α/β hydrolase essential for strigolactone signaling in Arabidopsis.
- 778 Plant Cell **26**:1134–1150.

- 779 **Conn, C. E., and Nelson, D. C.** (2015). Evidence that KARRIKIN-INSENSITIVE2 780 (KAI2) Receptors may Perceive an Unknown Signal that is not Karrikin or 781 Strigolactone. *Front. Plant Sci.* **6**:1219.
- Cook, C. E., Whichard, L. P., Turner, B., Wall, M. E., and Egley, G. H. (1966).
 Germination of Witchweed (Striga lutea Lour.): Isolation and Properties of a Potent Stimulant. *Science* 154:1189–1190.
- Day, R. N., Periasamy, A., and Schaufele, F. (2001). Fluorescence resonance energy transfer microscopy of localized protein interactions in the living cell nucleus.
 Methods 25:4–18.
- de Saint Germain, A., Clavé, G., Badet-Denisot, M.-A., Pillot, J.-P., Cornu, D., Le Caer, J.-P., Burger, M., Pelissier, F., Retailleau, P., Turnbull, C., et al. (2016). An histidine covalent receptor and butenolide complex mediates strigolactone perception. *Nat. Chem. Biol.* **12**:787–794.
- Flematti, G. R., Ghisalberti, E. L., Dixon, K. W., and Trengove, R. D. (2004). A compound from smoke that promotes seed germination. *Science* **305**:977.
- Flematti, G. R., Scaffidi, A., Waters, M. T., and Smith, S. M. (2016). Stereospecificity in strigolactone biosynthesis and perception. *Planta* **243**:1361–1373.
- Fujii, H., Verslues, P. E., and Zhu, J.-K. (2011). Arabidopsis decuple mutant reveals
 the importance of SnRK2 kinases in osmotic stress responses in vivo. *Proc. Natl.* Acad. Sci. U. S. A. 108:1717–1722.
- Gietz, R. D., and Woods, R. A. (2002). Transformation of yeast by lithium acetate/single-stranded carrier DNA/polyethylene glycol method. *Methods Enzymol.* **350**:87–96.
- Goddard-Borger, E. D., Ghisalberti, E. L., and Stick, R. V. (2007). Synthesis of the
 Germination Stimulant 3-Methyl-2H-furo[2,3-c]pyran-2-one and Analogous
 Compounds from Carbohydrates. *ChemInform* 38.
- Gomez-Roldan, V., Fermas, S., Brewer, P. B., Puech-Pagès, V., Dun, E. A., Pillot,
 J.-P., Letisse, F., Matusova, R., Danoun, S., Portais, J.-C., et al. (2008).
 Strigolactone inhibition of shoot branching. *Nature* 455:189–194.
- Haider, I., Andreo-Jimenez, B., Bruno, M., Bimbo, A., Floková, K., Abuauf, H., Ntui,
 V. O., Guo, X., Charnikhova, T., Al-Babili, S., et al. (2018). The interaction of
 strigolactones with abscisic acid during the drought response in rice. *J. Exp. Bot.*69:2403–2414.
- Hamiaux, C., Drummond, R. S. M., Janssen, B. J., Ledger, S. E., Cooney, J. M.,
 Newcomb, R. D., and Snowden, K. C. (2012). DAD2 is an α/β hydrolase likely to be involved in the perception of the plant branching hormone, strigolactone. *Curr. Biol.* 22:2032–2036.

- 816 Hu, Q., He, Y., Wang, L., Liu, S., Meng, X., Liu, G., Jing, Y., Chen, M., Song, X.,
- Jiang, L., et al. (2017). DWARF14, A Receptor Covalently Linked with the Active
- Form of Strigolactones, Undergoes Strigolactone-Dependent Degradation in Rice.
- 819 Front. Plant Sci. **8**:1935.
- Jain, N., Kulkarni, M. G., and van Staden, J. (2006). A butenolide, isolated from
- smoke, can overcome the detrimental effects of extreme temperatures during
- tomato seed germination. *Plant Growth Regul.* **49**:263–267.
- 823 Jiang, L., Liu, X., Xiong, G., Liu, H., Chen, F., Wang, L., Meng, X., Liu, G., Yu, H.,
- Yuan, Y., et al. (2013). DWARF 53 acts as a repressor of strigolactone signalling in
- 825 rice. *Nature* **504**:401–405.
- 826 Kalliola, M., Jakobson, L., Davidsson, P., Pennanen, V., Waszczak, C.,
- Yarmolinsky, D., Zamora, O., Palva, E. T., Kariola, T., Kollist, H., et al. (2020).
- Differential role of MAX2 and strigolactones in pathogen, ozone, and stomatal
- responses. *Plant Direct* **4**:e00206.
- 830 Khosla, A., Rodriguez Furlan, C., Kapoor, S., Van Norman, J. M., and Nelson, D.
- 831 **C.** (2020a). A series of dual reporter vectors for ratiometric analysis of protein
- abundance in plants. *Plant Direct* **4**.
- 833 Khosla, A., Morffy, N., Li, Q., Faure, L., Chang, S. H., Yao, J., Zheng, J., Cai, M. L.,
- Stanga, J., Flematti, G. R., et al. (2020b). Structure–Function Analysis of SMAX1
- Reveals Domains That Mediate Its Karrikin-Induced Proteolysis and Interaction with
- 836 the Receptor KAI2. *Plant Cell* **32**:2639–2659.
- 837 Kobae, Y., Kameoka, H., Sugimura, Y., Saito, K., Ohtomo, R., Fujiwara, T., and
- Kyozuka, J. (2018). Strigolactone Biosynthesis Genes of Rice are Required for the
- Punctual Entry of Arbuscular Mycorrhizal Fungi into the Roots. *Plant Cell Physiol.*
- **59**:544–553.
- Kochanek, J., Long, R. L., Lisle, A. T., and Flematti, G. R. (2016). Karrikins Identified
- in Biochars Indicate Post-Fire Chemical Cues Can Influence Community Diversity
- and Plant Development. *PLoS One* **11**:e0161234.
- Lahari, Z., Ullah, C., Kyndt, T., Gershenzon, J., and Gheysen, G. (2019).
- Strigolactones enhance root-knot nematode (Meloidogyne graminicola) infection in
- rice by antagonizing the jasmonate pathway. *New Phytol.* **224**:454–465.
- Li, W., Nguyen, K. H., Chu, H. D., Van Ha, C., Watanabe, Y., Osakabe, Y., Leyva-
- González, M. A., Sato, M., Toyooka, K., Voges, L., et al. (2017). The karrikin
- receptor KAI2 promotes drought resistance in Arabidopsis thaliana. *PLoS Genet.*
- **13**:e1007076.
- Li, W., Nguyen, K. H., Tran, C. D., Watanabe, Y., Tian, C., Yin, X., Li, K., Yang, Y.,
- Guo, J., Miao, Y., et al. (2020a). Negative Roles of Strigolactone-Related SMXL6,
- 7 and 8 Proteins in Drought Resistance in Arabidopsis. *Biomolecules* **10**.

- 854 Li, W., Nguyen, K. H., Chu, H. D., Watanabe, Y., Osakabe, Y., Sato, M., Toyooka, K., Seo, M., Tian, L., Tian, C., et al. (2020b). Comparative functional analyses of 855 DWARF14 and KARRIKIN INSENSITIVE 2 in drought adaptation of Arabidopsis 856 857 thaliana. *Plant J.* **103**:111–127.
- 858 Liang, Y., Ward, S., Li, P., Bennett, T., and Leyser, O. (2016). SMAX1-LIKE7 Signals from the Nucleus to Regulate Shoot Development in Arabidopsis via Partially EAR 859 860 Motif-Independent Mechanisms. Plant Cell 28:1581–1601.
- 861 Liu, D., Li, W., Cheng, J., and Hou, L. (2014). Expression analysis and functional characterization of a cold-responsive gene COR15A from Arabidopsis thaliana. 862 863 Acta Physiol. Plant 36:2421–2432.
- 864 López-Ráez, J. A., Charnikhova, T., Gómez-Roldán, V., Matusova, R., Kohlen, W., De Vos, R., Verstappen, F., Puech-Pages, V., Bécard, G., Mulder, P., et al. 865 (2008). Tomato strigolactones are derived from carotenoids and their biosynthesis 866 867 is promoted by phosphate starvation. New Phytol. 178:863–874.
- Msanne, J., Lin, J., Stone, J. M., and Awada, T. (2011). Characterization of abiotic 868 869 stress-responsive Arabidopsis thaliana RD29A and RD29B genes and evaluation of 870 transgenes. Planta 234:97–107.
- 871 Nasir, F., Tian, L., Shi, S., Chang, C., Ma, L., Gao, Y., and Tian, C. (2019). 872 Strigolactones positively regulate defense against Magnaporthe oryzae in rice 873 (Oryza sativa). Plant Physiol. Biochem. 142:106-116.
- 874 **Nelson, D. C.** (2021). The mechanism of host-induced germination in root parasitic plants. Plant Physiol. 185:1353-1373. 875
- Nelson, D. C., Flematti, G. R., Riseborough, J.-A., Ghisalberti, E. L., Dixon, K. W., 876 and Smith, S. M. (2010). Karrikins enhance light responses during germination and 877 seedling development in Arabidopsis thaliana. Proc. Natl. Acad. Sci. U. S. A. 878 879 **107**:7095–7100.
- 880 Nelson, D. C., Scaffidi, A., Dun, E. A., Waters, M. T., Flematti, G. R., Dixon, K. W., Beveridge, C. A., Ghisalberti, E. L., and Smith, S. M. (2011). F-box protein 881 MAX2 has dual roles in karrikin and strigolactone signaling in Arabidopsis thaliana. 882 883 Proc. Natl. Acad. Sci. U. S. A. 108:8897-8902.
- Nelson, D. C., Flematti, G. R., Ghisalberti, E. L., Dixon, K. W., and Smith, S. M. 884 (2012). Regulation of seed germination and seedling growth by chemical signals 885 from burning vegetation. Annu. Rev. Plant Biol. 63:107-130. 886
- 887 Rasmussen, A., Mason, M. G., De Cuyper, C., Brewer, P. B., Herold, S., Agusti, J., 888 Geelen, D., Greb, T., Goormachtig, S., Beeckman, T., et al. (2012). 889 Strigolactones suppress adventitious rooting in Arabidopsis and pea. Plant Physiol.

890

158:1976–1987.

- Scaffidi, A., Waters, M. T., Sun, Y. K., Skelton, B. W., Dixon, K. W., Ghisalberti, E.
 L., Flematti, G. R., and Smith, S. M. (2014). Strigolactone Hormones and Their
 Stereoisomers Signal through Two Related Receptor Proteins to Induce Different
 Physiological Responses in Arabidopsis. *Plant Physiol.* 165:1221–1232.
- Seto, Y., Yasui, R., Kameoka, H., Tamiru, M., Cao, M., Terauchi, R., Sakurada, A., Hirano, R., Kisugi, T., Hanada, A., et al. (2019). Strigolactone perception and deactivation by a hydrolase receptor DWARF14. *Nat. Commun.* **10**:191.
- Shabek, N., Ticchiarelli, F., Mao, H., Hinds, T. R., Leyser, O., and Zheng, N. (2018).

 Structural plasticity of D3-D14 ubiquitin ligase in strigolactone signalling. *Nature*563:652–656.
- Shah, F. A., Wei, X., Wang, Q., Liu, W., Wang, D., Yao, Y., Hu, H., Chen, X., Huang,
 S., Hou, J., et al. (2020). Karrikin Improves Osmotic and Salt Stress Tolerance via
 the Regulation of the Redox Homeostasis in the Oil Plant Sapium sebiferum. Front.
 Plant Sci. 11:216.
- Soundappan, I., Bennett, T., Morffy, N., Liang, Y., Stanga, J. P., Abbas, A., Leyser,
 O., and Nelson, D. C. (2015). SMAX1-LIKE/D53 Family Members Enable Distinct
 MAX2-Dependent Responses to Strigolactones and Karrikins in Arabidopsis. *Plant Cell* 27:3143–3159.
- Stanga, J. P., Smith, S. M., Briggs, W. R., and Nelson, D. C. (2013). SUPPRESSOR
 OF MORE AXILLARY GROWTH2 1 controls seed germination and seedling
 development in Arabidopsis. *Plant Physiol.* 163:318–330.
- 912 **Stanga, J. P., Morffy, N., and Nelson, D. C.** (2016). Functional redundancy in the control of seedling growth by the karrikin signaling pathway. *Planta* **243**:1397–1406.
- Sun, X.-D., and Ni, M. (2011). HYPOSENSITIVE TO LIGHT, an alpha/beta fold protein,
 acts downstream of ELONGATED HYPOCOTYL 5 to regulate seedling de etiolation. *Mol. Plant* 4:116–126.
- 918 **Swarbreck, S. M., Guerringue, Y., Matthus, E., Jamieson, F. J. C., and Davies, J. M.**919 (2019). Impairment in karrikin but not strigolactone sensing enhances root skewing
 920 in Arabidopsis thaliana. *The Plant Journal* **98**:607–621.
- Toh, S., Holbrook-Smith, D., Stokes, M. E., Tsuchiya, Y., and McCourt, P. (2014).
 Detection of parasitic plant suicide germination compounds using a high-throughput
 Arabidopsis HTL/KAI2 strigolactone perception system. *Chem. Biol.* 21:988–998.
- 924 **Ueda, H., and Kusaba, M.** (2015). Strigolactone Regulates Leaf Senescence in Concert with Ethylene in Arabidopsis. *Plant Physiol.* **169**:138–147.
- 926 Umehara, M., Hanada, A., Yoshida, S., Akiyama, K., Arite, T., Takeda-Kamiya, N., 927 Magome, H., Kamiya, Y., Shirasu, K., Yoneyama, K., et al. (2008). Inhibition of

- shoot branching by new terpenoid plant hormones. *Nature* **455**:195–200.
- 929 Van Ha, C., Leyva-González, M. A., Osakabe, Y., Tran, U. T., Nishiyama, R.,
- 930 Watanabe, Y., Tanaka, M., Seki, M., Yamaguchi, S., Van Dong, N., et al. (2014).
- Positive regulatory role of strigolactone in plant responses to drought and salt
- 932 stress. *Proc. Natl. Acad. Sci. U. S. A.* **111**:851–856.
- 933 Villaécija-Aguilar, J. A., Hamon-Josse, M., Carbonnel, S., Kretschmar, A., Schmidt,
- 934 C., Dawid, C., Bennett, T., and Gutjahr, C. (2019). SMAX1/SMXL2 regulate root
- and root hair development downstream of KAI2-mediated signalling in Arabidopsis.
- 936 *PLoS Genet.* **15**:e1008327.
- 937 Walker, C. H., Siu-Ting, K., Taylor, A., O'Connell, M. J., and Bennett, T. (2019).
- 938 Strigolactone synthesis is ancestral in land plants, but canonical strigolactone
- 939 signalling is a flowering plant innovation. *BMC Biol.* **17**:70.
- 940 Wang, L., Wang, B., Jiang, L., Liu, X., Li, X., Lu, Z., Meng, X., Wang, Y., Smith, S.
- 941 M., and Li, J. (2015). Strigolactone Signaling in Arabidopsis Regulates Shoot
- Development by Targeting D53-Like SMXL Repressor Proteins for Ubiquitination
- 943 and Degradation. *Plant Cell* **27**:3128–3142.
- Wang, L., Waters, M. T., and Smith, S. M. (2018). Karrikin-KAI2 signalling provides
- Arabidopsis seeds with tolerance to abiotic stress and inhibits germination under
- conditions unfavourable to seedling establishment. *New Phytol.* **219**:605–618.
- 947 Wang, L., Wang, B., Yu, H., Guo, H., Lin, T., Kou, L., Wang, A., Shao, N., Ma, H.,
- **Xiong, G., et al.** (2020a). Transcriptional regulation of strigolactone signalling in
- 949 Arabidopsis. *Nature* **583**:277–281.
- 950 Wang, L., Xu, Q., Yu, H., Ma, H., Li, X., Yang, J., Chu, J., Xie, Q., Wang, Y., Smith,
- 951 **S. M., et al.** (2020b). Strigolactone and Karrikin Signaling Pathways Elicit
- Ubiquitination and Proteolysis of SMXL2 to Regulate Hypocotyl Elongation in
- 953 Arabidopsis. *Plant Cell* **32**:2251–2270.
- 954 Wang, Y., Yao, R., Du, X., Guo, L., Chen, L., Xie, D., and Smith, S. M. (2021).
- 955 Molecular basis for high ligand sensitivity and selectivity of strigolactone receptors
- 956 in Striga. *Plant Physiol.* **185**:1411–1428.
- 957 Waters, M. T., Nelson, D. C., Scaffidi, A., Flematti, G. R., Sun, Y. K., Dixon, K. W.,
- and Smith, S. M. (2012). Specialisation within the DWARF14 protein family confers
- 959 distinct responses to karrikins and strigolactones in Arabidopsis. *Development*
- 960 **139**:1285–1295.
- 961 Waters, M. T., Scaffidi, A., Moulin, S. L. Y., Sun, Y. K., Flematti, G. R., and Smith, S.
- 962 **M.** (2015a). A Selaginella moellendorffii ortholog of KARRIKIN INSENSITIVE2
- 963 functions in Arabidopsis development but cannot mediate responses to karrikins or
- 964 strigolactones. *Plant Cell* **27**:1925–1944.

- Waters, M. T., Scaffidi, A., Flematti, G., and Smith, S. M. (2015b). Substrate-Induced
 Degradation of the α/β-Fold Hydrolase KARRIKIN INSENSITIVE2 Requires a
 Functional Catalytic Triad but Is Independent of MAX2. *Mol. Plant* 8:814–817.
- Waters, M. T., Gutjahr, C., Bennett, T., and Nelson, D. C. (2017). Strigolactone
 Signaling and Evolution. *Annu. Rev. Plant Biol.* 68:291–322.
- White, A. R. F., Mendez, J. A., Khosla, A., and Nelson, D. C. (2021). Rapid analysis
 of strigolactone receptor activity in a *Nicotiana benthamiana dwarf14* mutant. *Biorxiv* Advance Access published May 11, 2021, doi:10.1101/2021.05.11.443507.
- Xu, Y., Miyakawa, T., Nosaki, S., Nakamura, A., Lyu, Y., Nakamura, H., Ohto, U.,
 Ishida, H., Shimizu, T., Asami, T., et al. (2018). Structural analysis of HTL and
 D14 proteins reveals the basis for ligand selectivity in Striga. *Nature* Communications 9.
- 977 Yamada, Y., Furusawa, S., Nagasaka, S., Shimomura, K., Yamaguchi, S., and 978 Umehara, M. (2014). Strigolactone signaling regulates rice leaf senescence in 979 response to a phosphate deficiency. *Planta* **240**:399–408.
- Yao, J.R., Scaffidi, A., Meng, Y.J., Melville, K.T., Komatsu, A., Khosla, A., Nelson,
 D.C., Kyozuka, J., Flematti, G.R., and Waters, M.T. (2021). Desmethyl
 butenolides are optimal ligands for karrikin receptor proteins. *New Phytol.* 230:1003-1016.
- Yao, R., Ming, Z., Yan, L., Li, S., Wang, F., Ma, S., Yu, C., Yang, M., Chen, L., Chen,
 L., et al. (2016). DWARF14 is a non-canonical hormone receptor for strigolactone.
 Nature 536:469–473.
- Yao, R., Wang, F., Ming, Z., Du, X., Chen, L., Wang, Y., Zhang, W., Deng, H., and
 Xie, D. (2017). ShHTL7 is a non-canonical receptor for strigolactones in root
 parasitic weeds. *Cell Res.* 27:838–841.
- Yoneyama, K., Mori, N., Sato, T., Yoda, A., Xie, X., Okamoto, M., Iwanaga, M.,
 Ohnishi, T., Nishiwaki, H., Asami, T., et al. (2018). Conversion of carlactone to
 carlactonoic acid is a conserved function of MAX1 homologs in strigolactone
 biosynthesis. New Phytol. 218:1522–1533.
- Zheng, J., Hong, K., Zeng, L., Wang, L., Kang, S., Qu, M., Dai, J., Zou, L., Zhu, L.,
 Tang, Z., et al. (2020). Karrikin Signaling Acts Parallel to and Additively with
 Strigolactone Signaling to Regulate Rice Mesocotyl Elongation in Darkness. *Plant Cell* 32:2780–2805.
- Zheng, X., Yang, X., Chen, Z., Xie, W., Yue, X., Zhu, H., Chen, S., and Sun, X.
 (2021). Arabidopsis SMAX1 overaccumulation suppresses rosette shoot branching and promotes leaf and petiole elongation. *Biochem. Biophys. Res. Commun.* 553:44–50.

Zhou, F., Lin, Q., Zhu, L., Ren, Y., Zhou, K., Shabek, N., Wu, F., Mao, H., Dong, W.,
 Gan, L., et al. (2013). D14-SCF(D3)-dependent degradation of D53 regulates
 strigolactone signalling. *Nature* 504:406–410.

- 1005 **FIGURE LEGENDS**
- 1006 Figure 1. D14 inhibits hypocotyl growth after GR24 treatment via SMAX1 and
- 1007 **SMXL2**.
- Hypocotyl lengths of 5-d-old seedlings of Col-0, *kai2*, *d14-1*, *kai2 d14-1*, *smax1 smxl2*,
- 1009 kai2 smax1 smxl2, d14-1 smax1 smxl2, smxl 6,7,8, kai2 smxl6,7,8 and d14-1 smxl6,7,8
- 1010 grown under continuous red light for 4 d on the 0.5x MS agar media containing 1 µM
- 1011 KAR₂, 1 μ M *rac*-GR24 or acetone. Bar = 5 mm. Box-and-whisker plots with the same
- letter are not significantly different from one another (Tukey HSD, p < 0.05, n \geq 30).

1013

- 1014 Figure 2. SMAX1 is the primary regulator of hypocotyl responses to KAI2- and D14-
- 1015 **mediated signaling.**
- Hypocotyl lengths of 5-d-old seedlings of Col-0, *kai2*, *d14-1*, *smax1*, *smxl2*, *kai2 smax1*,
- 1017 d14-1 smax1, kai2 smxl2, d14-1 smxl2 grown under continuous red light for 4 d on the
- 1018 0.5x MS media containing 1 µM KAR₂,1 µM *rac*-GR24 or acetone. Box-and-whisker plots
- with the same letter are not significantly different from one another (Tukey HSD, p < 0.05,
- 1020 $n \ge 30$).

- Figure 3. SL triggers SMAX1 and SMXL2 degradation through D14.
- 1023 Relative fluorescence from the SMAX1-mScarlet-l reporter (A) or SMXL2-mScarlet-l
- reporter (**B**) or SMAX1_{D2}-mScarlet-I reporter (**C**) and the Venus reference after transient
- expression of the ratiometric system in wt tobacco and *Nbd14* is shown. Leaf discs are
- 1026 treated with acetone, 10 μM KAR₁, or 10 μM GR24^{5DS} for 12 h before measurement. n =
- 1027 5-8 leaf discs. Asterisks indicate significant differences from each acetone control or
- between compared pairs using the Student's t-test (*p < 0.05 and **p < 0.01).
- 1029 Relative fluorescence from the SMAX1-mScarlet-I reporter (D) or SMXL7-mScarlet-I
- reporter (E) along with D14, d14^{seto}, d14^{S97A} or empty vector (EV) expressed in *Nbd14* at
- 1031 0 h, 1h, and 2 h after 10 μ M GR24^{5DS} treatment. n = 12 leaf discs. ns indicates no
- 1032 significance. *p < 0.05, **p < 0.01, Student's t-test comparisons to the relative
- 1033 fluorescence at 0 h or between compared pairs.
- SMAX1_{D2}-LUC transgenic seedlings in the Col-0, *kai2*, *d14-1* and *max2* backgrounds are
- treated with 5 μM KAR₂ (**F**), 5 μM GR24^{5DS} (**G**) or acetone for 4 h. Bioluminescence is

shown as relative LUC activity at 0 h, 2 h and 4h after treatment. n = 12-14 seedlings. *p < 0.05, **p < 0.01, Student's t-test comparisons to each genotype/treatment at 0 h.

- 1039 Figure 4. D14 and SMAX1 proteins can physically interact.
- 1040 (A) Yeast two-hybrid assays for D14 and d14^{seto} interactions with SMAX1, SMXL7 and
- their D1M domains. D14 and d14^{seto} are fused to GAL4-BD. SMAX1, SMXL7 and their
- domains are fused to GAL4-AD. Serial 10-fold dilutions of yeast cultures are spotted onto
- selective growth medium (-L, -Leu; -T, -Trp; -H, -His; -A, -Ade) that is supplemented with
- 1044 2 μM GR24^{5DS} or acetone control.
- 1045 Split-luciferase complementation assay for interactions between SMXL7 (B),
- 1046 SMAX1^{ΔRGKT} (C), SMXL2 (D) and D1M domains of SMAX1 (E) and SMXL7 (F) with D14,
- 1047 d14^{seto} or d14^{S97A}. *N. benthamiana* leaves are transiently co-transformed with
- 1048 Agrobacterium tumefaciens strains carrying cLUC, nLUC, or indicated fusions as well as
- 1049 a strain carrying an mCherry transgene as a transformation control. Luminescence is
- measured before and 1 hour after treatment with 10 µM GR24^{5DS}, and normalized against
- mCherry fluorescence. Box-and-whisker plots with the same letter are not significantly
- different from one another (Student's t, p < 0.05, n = 7-15 leaf discs).
- 1053 **(G)** FRET-ABP assay for interactions between SMAX1 with D14. *N. benthamiana* leaves
- are transiently co-transformed with Agrobacterium tumefaciens strains carrying SMAX1-
- 1055 GFP-mCherry or indicated fusions. The FRET efficiency is shown as the percentage that
- 1056 donor fluorescence increases compared with that before receptor bleaching. + (dark
- 1057 green box) and (white box) indicate SMAX1-GFP-mCherry as a positive control and
- 1058 SMAX1-mCherry/Myc-GFP pair as a negative control, respectively. Acetone-treated leaf
- 1059 discs are used as mock control. Box-and-whisker plots with the same letter are not
- significantly different from one another (Student's t, p < 0.05, n = 6-21 leaf discs).
- 1061 **(H)** FRET-ABP assay for interactions between SMXL7 with D14. *N. benthamiana* leaves
- are transiently co-transformed with Agrobacterium tumefaciens strains carrying SMXL7-
- 1063 GFP-mCherry or indicated fusions. + (dark green box) and (white box) indicate SMXL7-
- 1064 GFP-mCherry as a positive control and SMXL7-mCherry/Myc-GFP pair as a negative
- 1065 control, respectively. Acetone-treated leaf discs are used as mock control. Box-and-

- 1066 whisker plots with the same letter are not significantly different from one another
- 1067 (Student's t, p < 0.05, n = 6-18 leaf discs).

1068

- 1069 Figure 5. d14^{seto} is hypomorphic and more active in a smax1 smx12 background.
- 1070 **(A)** Adult shoot morphology of Col-0 (wild type), d14-1, kai2 d14-1, d14-1 smax1, d14-1
- 1071 smax1 smxl2, d14seto, kai2 d14seto, d14seto smax1, d14seto smax1 smxl2, d14seto smax1
- 1072 smx/2 max 2 and max 2 plants. Bar = 5 cm.
- 1073 **(B)** The number of Primary rosette branches of plant materials in **(A)**. Box-and-whisker
- plots with the same letter are not significantly different from one another (Tukey HSD, P
- 1075 < 0.05, n = 21 to 34).
- 1076 **(C)** RT-qPCR analysis of *BRC1/TCP18* gene expression in non-elongated axillary buds
- 1077 of Col-0, d14-1, kai2 d14-1, d14-1 smax1 smxl2, d14^{seto}, kai2 d14^{seto}, d14^{seto} smax1 smxl2,
- 1078 d14^{seto} smax1 smxl2 max2 and max2 plants collected 10 d after anthesis. Expression of
- 1079 BRC1 is relative to CACS internal reference gene. Scatter dot plots with the same letter
- are not significantly different from one another (bar indicates mean; n = 4 pooled tissue
- samples, 3 plants per pool; Student's t, p < 0.05).

- 1083 Figure 6. D14 degradation after GR24^{5DS} treatment is enhanced by SMAX1 and
- 1084 **SMXL2**
- 1085 **(A)** Relative GFP signal from *D14-GFP* or *d14*^{seto}-*GFP* transgenic plant is measured every
- 1086 10 minutes in the presence of 5 µM *rac-*GR24. The curve is generated from the mean
- 1087 value per genotype/treatment at each time point. Bar indicates standard error of the mean
- 1088 (n = 6 seedlings).
- 1089 **(B)** UBQ:D14-LUC transgenic seedlings in the Col-0 and smax1 smxl2 backgrounds are
- 1090 treated with 5 μM GR24^{5DS} or acetone for 12 h. Bioluminescence is shown as relative
- 1091 LUC activity at 0 h, 2 h, 4 h, 8 h and 12 h after treatment. n = 10-12 seedlings. Asterisks
- indicate significant differences to each group at 0 h or between compared pairs using the
- Student's t-test (*p < 0.05 and **p < 0.01; ns indicates no significance).
- 1094 (C) Time course assay of D14, d14^{seto} and d14^{S97A} stability in *N. benthamiana* under 10
- 1095 µM GR24^{5DS} treatment. Relative fluorescence from the D14-mScarlet-I reporter, d14^{seto}-
- mScarlet-I reporter or d14^{S97A}-mScarlet-I reporter and the Venus reference after transient

- 1097 co-expression of the ratiometric system and SMAX1 effector in tobacco is shown. Leaf
- discs are treated for 12 h to monitor D14, d14^{seto} and d14^{S97A} stability. n = 14 leaf discs.
- 1099 Asterisks indicate significant differences to each group at 0 h or between compared pairs
- using the Student's t-test (*p < 0.05 and **p < 0.01; ns indicates no significance).

1101

- 1102 Figure 7. D14 targets SMAX1 and SMXL2 under osmotic stress.
- 1103 **(A)** 21-day-old seedlings of Col-0, *smax1 smxl2*, *smxl* 6,7,8, *d14-1*, *d14-1 smax1 smxl2*,
- 1104 d14-1 smxl6,7,8, kai2, kai2 smax1 smxl2 and kai2 smxl6,7,8 grown in mock or 300 mM
- 1105 mannitol condition for 14 days. Bar = 2 cm.
- 1106 **(B)** Relative fresh weights of plant materials used in **(A)** to application of 300 mM mannitol.
- 1107 The weights of aerial parts from plants grown on 0.5x MS agar medium containing 300
- 1108 mM mannitol are scaled to that from plants grown on 0.5x MS agar medium. Scatter dot
- plots with the same letter are not significantly different from one another (bar indicates
- 1110 mean; n = 4; Student's t, p < 0.05).
- 1111 **(C)** Chlorophyll (Chl) contents in the aerial parts of Arabidopsis seedlings used in **(A)**.
- 1112 Others are as in (B).
- 1113 **(D)** Bioluminescence of SMAX1_{D2}-LUC in Col-0, *kai2*, *d14-1*, *max2* and *max3*
- 1114 backgrounds. Seedlings were treated with 300 mM mannitol or water control for 12 h.
- 1115 Bioluminescence is shown as relative LUC activity at 0 h, 4 h, 8 h and 12 h after treatment.
- 1116 n = 16-18 seedlings. ns indicates no significance. *p < 0.05, **p < 0.01, Student's t-test
- 1117 comparisons to Col-0 control at each time point.
- 1118 **(E)** Expression of *RD29A*, *Cor15A* and *PKS5* relative to CACS internal reference in Col-
- 1119 0, smax1 smxl2 and smxl6,7,8 grown 7 d under a long-day photoperiod (16 h light/8 h
- dark) after 3 h mock or 300 mM mannitol treatment. Scatter dot plots with the same letter
- are not significantly different from one another (bar indicates mean; n = 3; Student's t, p
- 1122 < 0.05).

1123

- 1124 Figure 8. Model for crosstalk between SL and KAR/KL signaling pathways.
- 1125 KAI2 recruits the SCF^{MAX2} E3 ubiquitin ligase complex upon perception of KAR/KL or
- 1126 GR24^{ent-5DS} to target SMAX1 and SMXL2 for degradation. SL or GR24^{5DS} induces
- association of D14 with SCF^{MAX2} and SMXL7, SMXL2, and, to a weaker extent, SMAX1.

This subsequently causes MAX2-dependent degradation of the targets. GR24^{ent-5DS} activates D14 more weakly than GR24^{5DS}. GR24^{5DS} may trigger KAI2 signaling to a weak degree (dotted line), although evidence of ligand-binding and *in vitro* activation is missing. Degradation of SMXL7 represses shoot branching, whereas degradation of SMAX1 represses seed germination and hypocotyl elongation. SMXL2 plays a minor role in hypocotyl elongation compared to SMAX1. In seedlings, endogenous SL is insufficient to trigger crosstalk between D14 and SMAX1. It occurs, however, in the presence of GR24 and in some conditions such as osmotic stress that might raise SL levels.

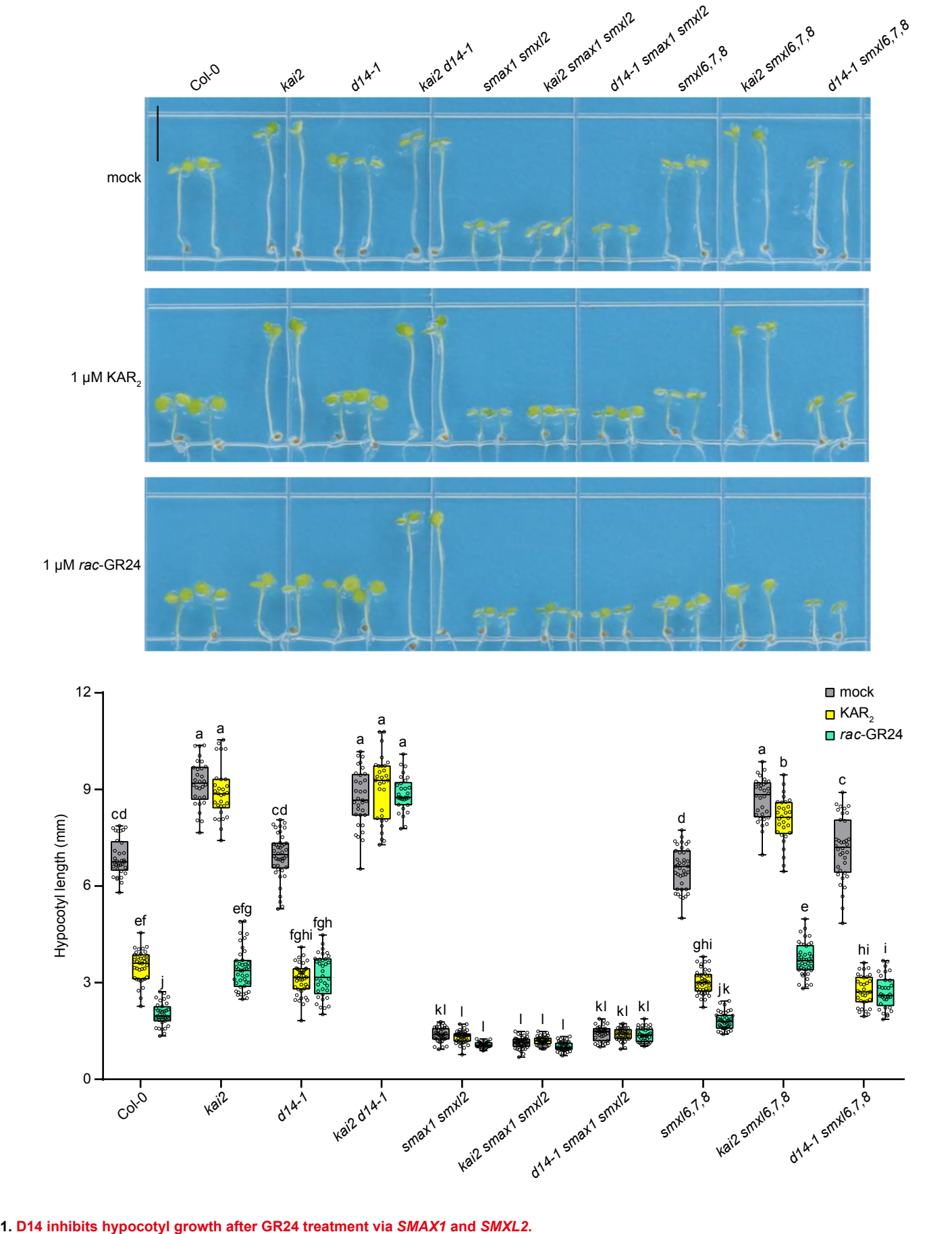


Fig. 1. D14 inhibits hypocotyl growth after GR24 treatment via SMAX1 and SMXL2. Hypocotyl lengths of 5-d-old seedlings of Col-0, kai2, d14-1, kai2 d14-1, smax1 smx12, kai2 smax1 smx12, d14-1 smax1 smx12, smx1 6,7,8, kai2 smx16,7,8 and d14-1 smax1 smx16,7,8 grown under continuous red light for 4 d on the 0.5x MS agar media containing 1 μ M KAR₂, 1 μ M rac-GR24 or acetone. Bar = 5 mm. Box-and-whisker plots with the same letter are not significantly different from one another (Tukey HSD, p < 0.05, n \geq 30).

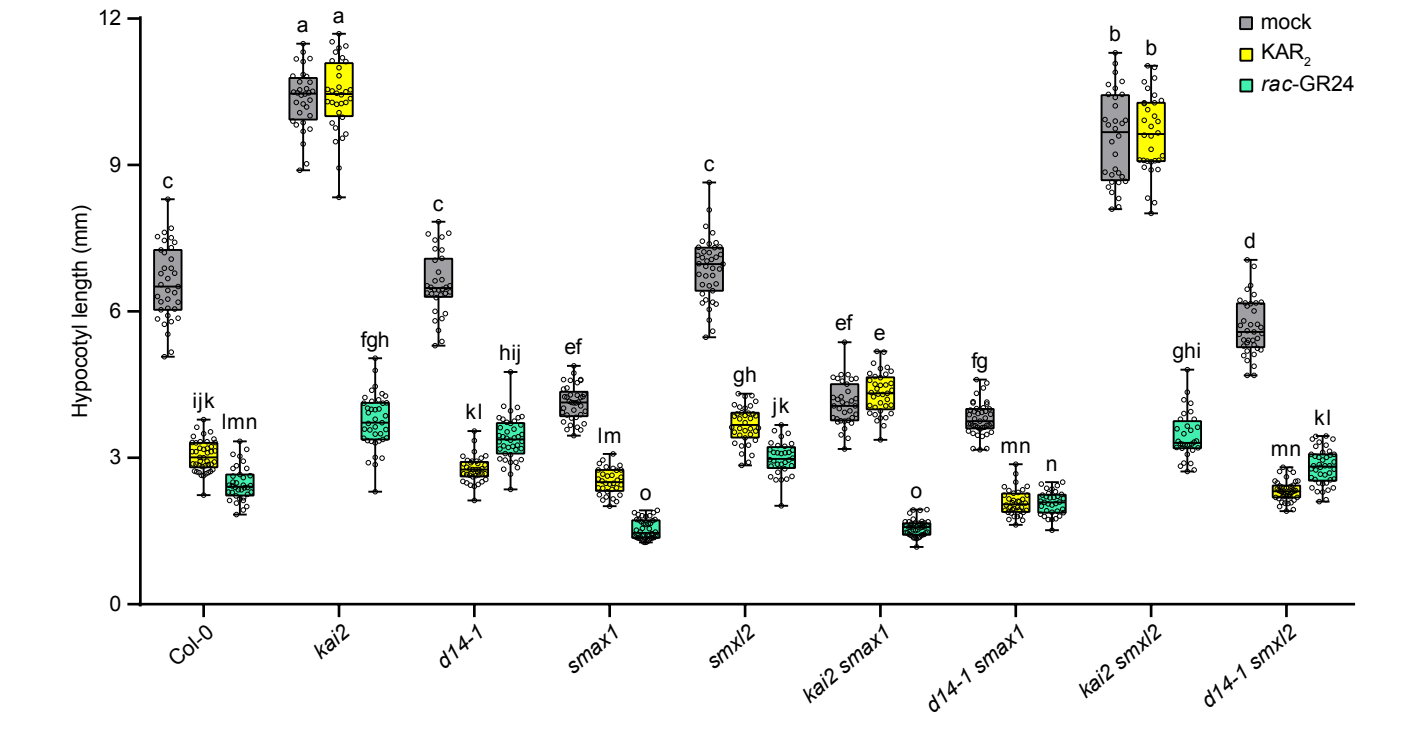


Fig. 2. SMAX1 is the primary regulator of hypocotyl responses to KAI2- and D14-mediated signaling. Hypocotyl lengths of 5-d-old seedlings of CoI-0, kai2, d14-1, smax1, smx12, kai2, d14-1, smax1, kai2, d14-1, smax12, d14-1, d14-1

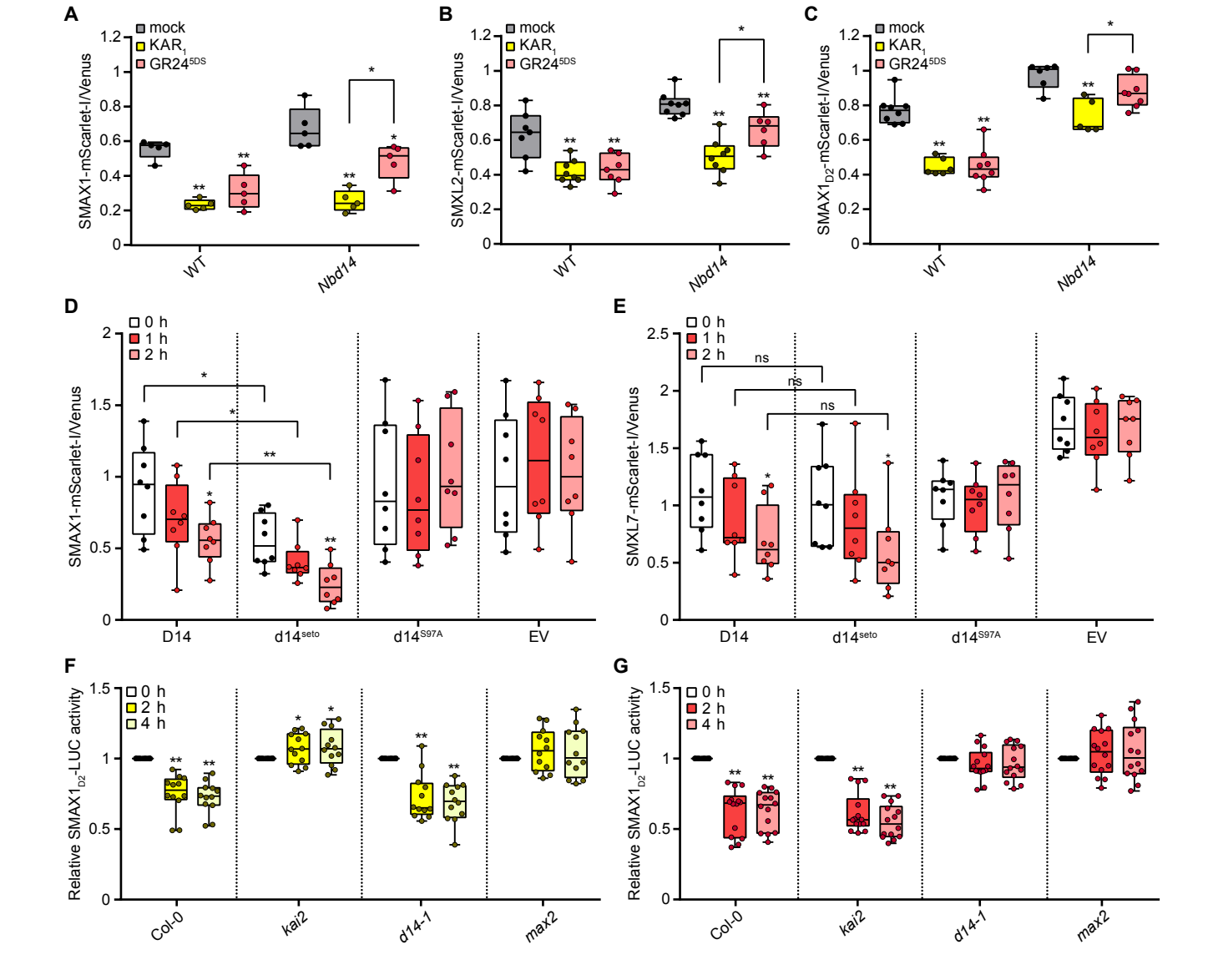


Fig. 3. SL triggers SMAX1 and SMXL2 degradation through D14.

Relative fluorescence from the SMAX1-mScarlet-I reporter (A) or SMXL2-mScarlet-I reporter (B) or SMAX

Relative fluorescence from the SMAX1-mScarlet-I reporter **(A)** or SMXL2-mScarlet-I reporter **(B)** or SMAX1_{D2}-mScarlet-I reporter **(C)** and the Venus reference after transient expression of the ratiometric system in wt tobacco and *Nbd14* is shown. Leaf discs are treated with acetone, 10 μ M KAR₁, or 10 μ M GR24^{5DS} for 12 h before measurement. n = 5-8 leaf discs. Asterisks indicate significant differences from each acetone control or between compared pairs using the student's t test (*p < 0.05 and **p < 0.01).

Relative fluorescence from the SMAX1-mScarlet-I reporter **(D)** or SMXL7-mScarlet-I reporter **(E)** along with D14, d14^{seto}, d14^{se}

SMAX1_{D2}-LUC2 transgenic seedlings in the Coi-0, *kai2*, *d14-1* and *max2* backgrounds are treated with 5 μ M KAR₂ (**F**), 5 μ M GR24^{5DS} (**G**) or acetone for 4 h. Bioluminescence is shown as relative LUC activity at 0 h, 2 h and 4h after treatment. n = 12-14 seedlings. *p < 0.05, **p < 0.01, student's t test comparisons to each genotype/treatment at 0 h.

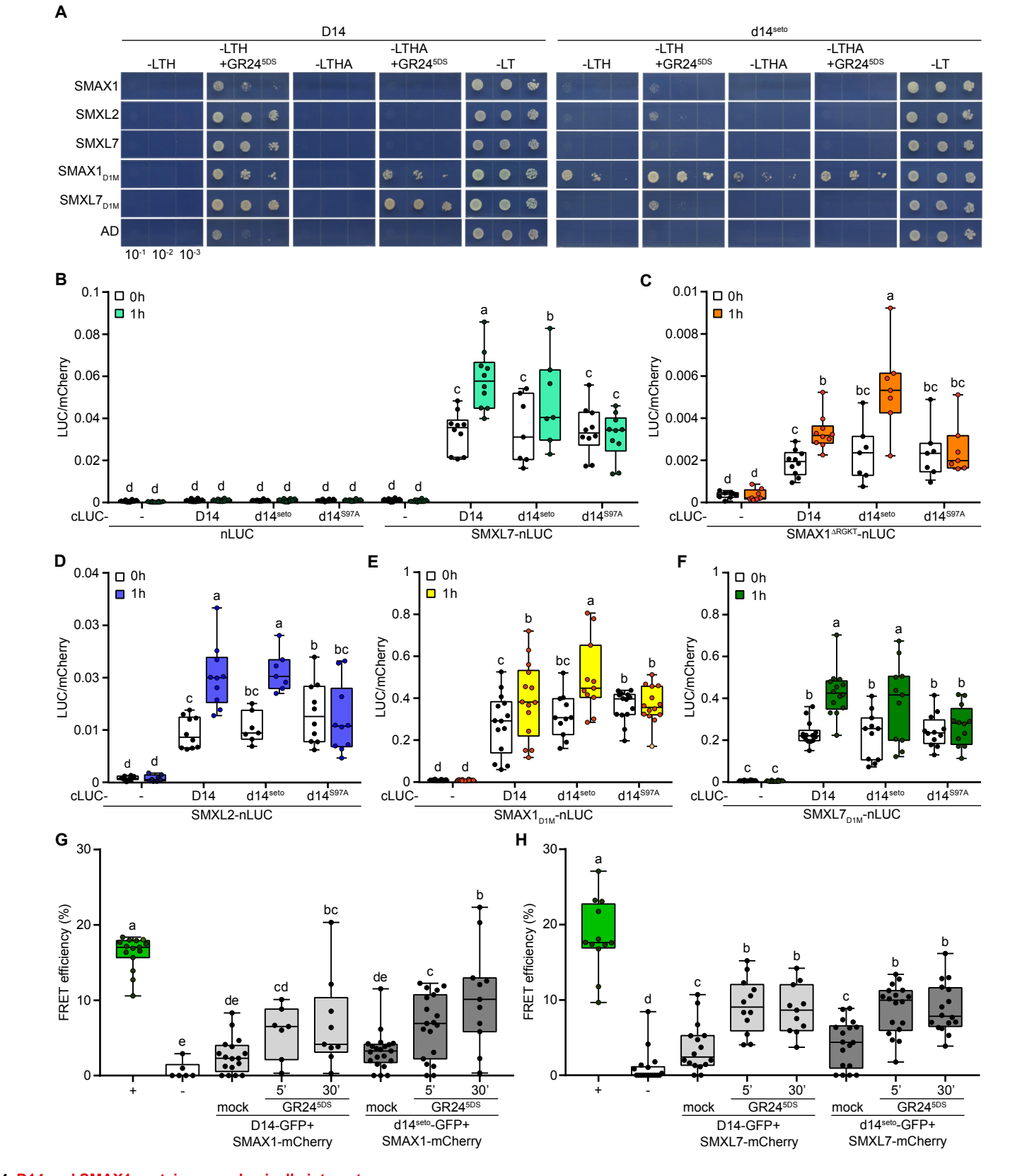


Fig. 4. D14 and SMAX1 proteins can physically interact.
(A) Yeast two-hybrid assays for D14 and d14^{seto} interactions with SMAX1, SMXL7 and their D1M domains. D14 and d14^{seto} are fused to GAL4-BD. SMAX1, SMXL7 and their domains are fused to GAL4-AD. Serial 10-fold dilutions of yeast cultures are spotted onto selective growth medium (-L, -Leu; -T, -Trp; -H, -His; -A, -Ade) that is supplemented with 2 μM GR24^{5DS} or acetone control.

Split-luciferase complementation assay for interactions between SMXL7 (**B**), SMAX1^{ΔRGKT} (**C**), SMXL2 (**D**) and D1M domains of SMAX1 (**E**) and SMXL7 (**F**) with D14, d14^{seto} or d14^{S97A}. *N. benthamiana* leaves are transiently co-transformed with *Agrobacterium tumefaciens* strains carrying cLUC, nLUC, or indicated fusions as well as a strain carrying an mCherry transgene as a transformation control. Luminescence is measured before and 1 hour after treatment with 10 μM GR24^{5DS}, and normalized against mCherry fluorescence. Box-and-whisker plots with the same letter are not significantly different from one another (student's t, p < 0.05, n = 7-15 leaf discs). (**G**) FRET-ABP assay for interactions between SMAX1 with D14. *N. benthamiana* leaves are transiently co-transformed with *Agrobacterium tumefaciens* strains carrying SMAX1-GFP-mCherry or indicated fusions. The FRET efficiency is shown as the percentage that donor fluorescence increases compared with that before receptor bleaching. + (dark green box) and - (white box) indicate SMAX1-GFP-mCherry as a positive control and SMAX1-mCherry/Myc-GFP pair as a negative control, respectively. Acetone-treated leaf discs are used as mock control. Box-and-whisker plots with the same letter are not significantly different from one another (student's t, p < 0.05, n = 6-21 leaf discs).

(H) FRET-ABP assay for interactions between SMXL7 with D14. *N. benthamiana* leaves are transiently co-transformed with *Agrobacterium tumefaciens* strains carrying SMXL7-GFP-mCherry or indicated fusions. + (dark green box) and - (white box) indicate SMXL7-GFP-mCherry as a positive control and SMXL7-mCherry/Myc-GFP pair as a negative control, respectively. Acetone-treated leaf discs are used as mock control. Box-and-whisker plots with the same letter are not significantly different from one another (student's t, p < 0.05, n = 6-18 leaf discs).

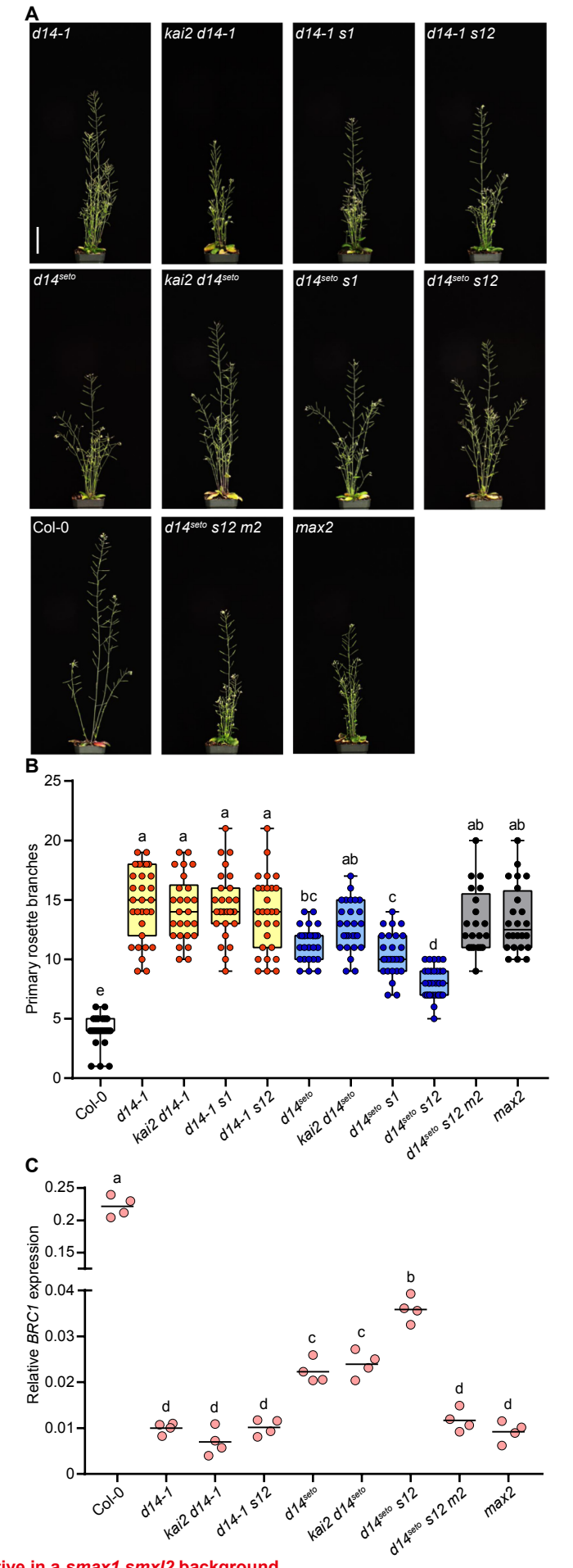
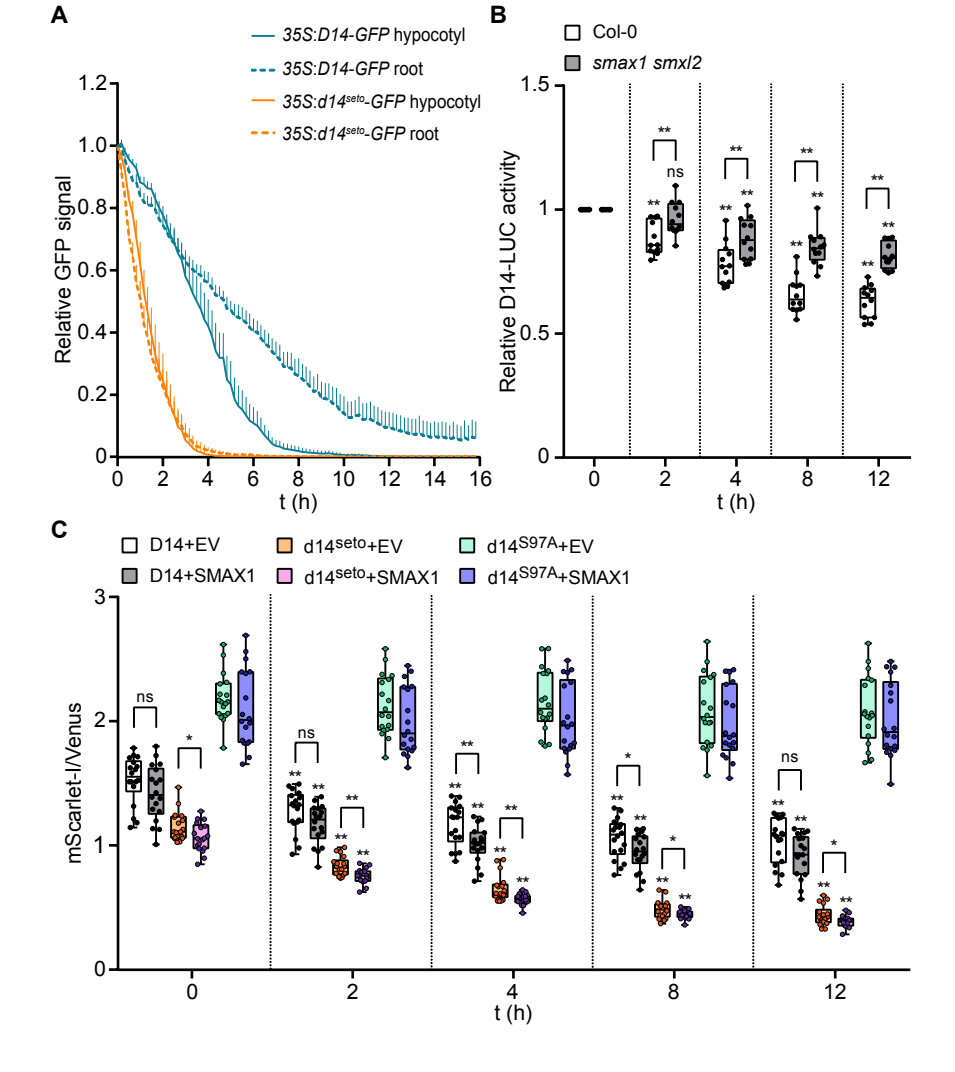


Fig. 5. d14^{seto} is hypomorphic and more active in a smax1 smx/2 background.

(A) Adult shoot morphology of Col-0 (wild type), d14-1, kai2 d14-1, d14-1 smax1, d14-1 smax1 smx/2, d14^{seto}, kai2 d14^{seto}, d14^{seto} smax1, d14^{seto} smax1 smx/2, d14^{seto} smax1 smx/2 max2 and max2 plants. Bar = 5 cm.

⁽B) The number of Primary rosette branches of plant materials in **(A)**. Box-and-whisker plots with the same letter are not significantly different from one another (Tukey HSD, p < 0.05, n = 21 to 34).

⁽C) RT-qPCR analysis of *BRC1/TCP18* gene expression in non-elongated axillary buds of Col-0, *d14-1*, *kai2 d14-1*, *d14-1 smax1 smxl2*, *d14*^{seto}, *kai2 d14*^{seto}, *d14*^{seto} smax1 smxl2, *d14*^{seto} smax1 smxl2 max2 and max2 plants collected 10 d after anthesis. Expression of *BRC1* is relative to *CACS* internal reference gene. Scatter dot plots with the same letter are not significantly different from one another (bar indicates mean; n = 4 pooled tissue samples, 3 plants per pool; student's t, p < 0.05).



(A) Relative GFP signal from *D14-GFP* or *d14*^{seto}-*GFP* transgenic plant is measured every 10 minutes in the presence of 5 µM *rac*-GR24. The curve is generated from the mean value per treatment/genotype at each time point. Bar indicates standard error of the mean (n = 6 seedlings).

Fig. 6. D14 degradation after GR24^{5DS} treatment is enhanced by SMAX1 and SMXL2.

(B) UBQ:D14-LUC transgenic seedlings in the Col-0 and smax1 smxl2 backgrounds are treated with 5 μ M GR24^{5DS} or acetone for 12 h. Bioluminescence is shown as relative LUC activity at 0 h, 2 h, 4 h, 8 h and 12 h after treatment. n = 10-12 seedlings. Asterisks indicate significant differences to each group at 0 h or between compared pairs using the student's t test (*p < 0.05 and **p < 0.01; ns indicates no significance).

(C) Time course assay of D14, d14seto and d14seto and

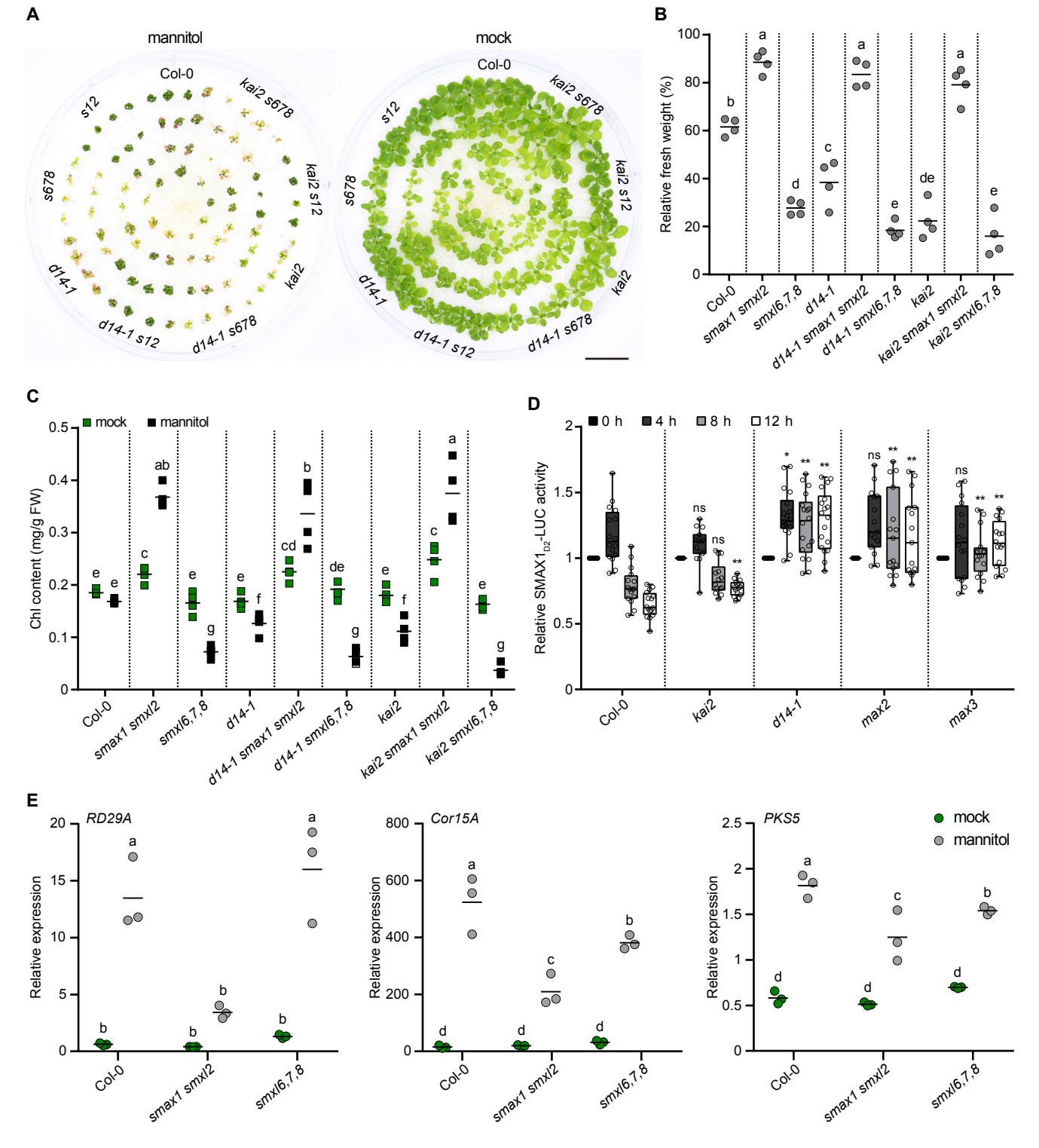


Fig. 7. D14 targets SMAX1 and SMXL2 under osmotic stress.

(A) 21-day-old seedlings of Col-0, smax1 smx/2, smx/1 6,7,8, d14-1, d14-1 smax1 smx/12, d14-1 smx/16,7,8, kai2, kai2 smax1 smx/12 and kai2 smx/16,7,8 grown in mock or 300 mM mannitol condition for 14 days. Bar = 2 cm.

- **(B)** Relative fresh weights of plant materials used in **(A)** to application of 300 mM mannitol. The weights of aerial parts from plants grown on 0.5x MS agar medium containing 300 mM mannitol are scaled to that from plants grown on 0.5x MS agar medium. Scatter dot plots with the same letter are not significantly different from one another (bar indicates mean; n = 4; student's t, p < 0.05).
- (C) Chlorophyll (Chl) contents in the aerial parts of Arabidopsis seedlings used in (A). Others are as in (B).
- (**D**) Bioluminescence of SMAX1_{D2}-LUC2 in Col-0, kai2, d14-1, max2 and max3 backgrounds. Seedlings were treated with 300 mM mannitol or water control for 12 h. Bioluminescence is shown as relative LUC activity at 0 h, 4 h, 8 h and 12 h after treatment. n = 16-18 seedlings. ns indicates no significance. *p < 0.05, **p < 0.01, student's t test comparisons to Col-0 control at each time point.

(E) Expression of *RD29A*, *Cor15A* and *PKS5* relative to *CACS* internal reference in Col-0, *smax1 smxl2* and *smxl6,7,8* grown 7 d under a long-day photoperiod (16 h light/8 h dark) after 3 h mock or 300 mM mannitol treatment. Scatter dot plots with the same letter are not significantly different from one another (bar indicates mean; n = 3; student's t, p < 0.05).

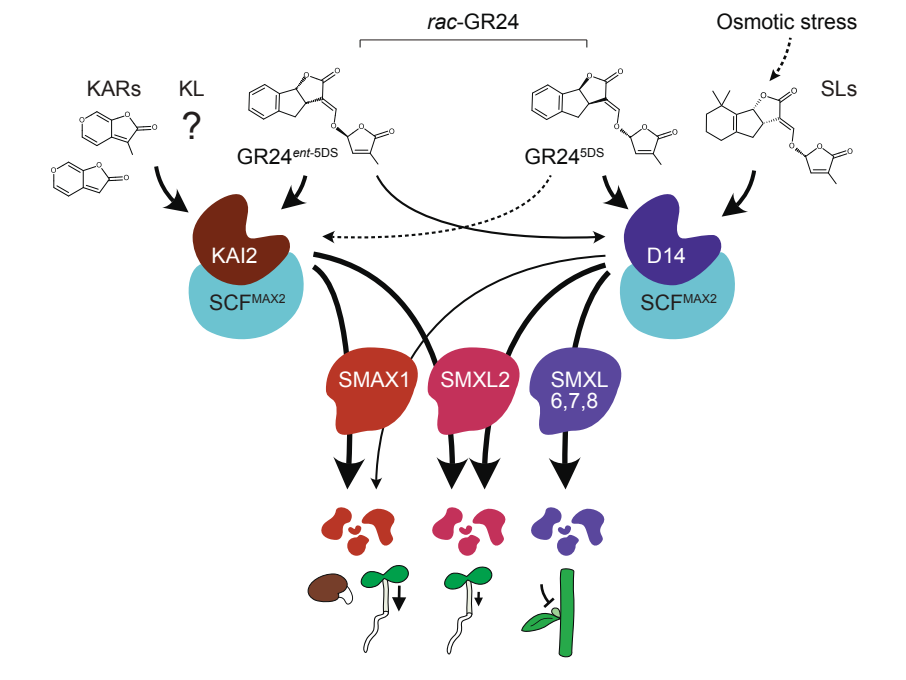


Fig. 8. Model for crosstalk between SL and KAR/KL signaling.

KAI2 recruits the SCF^{MAX2} E3 ubiquitin ligase complex upon perception of KAR/KL or GR24^{ent-5DS} to target SMAX1 and SMXL2 for degradation. SL or GR24^{5DS} induces association of D14 with SCF^{MAX2} and SMXL7, SMXL2, and, to a weaker extent, SMAX1. This subsequently causes MAX2-dependent degradation of the targets. GR24^{ent-5DS} activates D14 more weakly than GR24^{5DS}. GR24^{5DS} may trigger KAI2 signaling to a weak degree (dotted line), although evidence of ligand-binding and *in vitro* activation is missing. Degradation of SMXL7 represses shoot branching, whereas degradation of SMAX1 represses seed germination and hypocotyl elongation. SMXL2 plays a minor role in hypocotyl elongation compared to SMAX1. In seedlings, endogenous SL is insufficient to trigger crosstalk between D14 and SMAX1. It occurs, however, in the presence of GR24 and in some conditions such as osmotic stress that might raise SL levels.

Supplemental Information text

Extended Description of Materials and Methods

Plant growth conditions

Plants were grown under white light (MaxLite LED T8 4000K, ~110 μmol m⁻² s⁻¹) with LD photoperiod (16 h light/8 h dark) at 21°C. Soil was supplemented with Gnatrol WDG and Marathon (imidacloprid). *Agrobacterium tumefaciens* (GV3101 pMP90)–mediated transformation of *Arabidopsis* was performed using the floral dip method as described previously (Clough and Bent, 1998). All characterized transgenic lines were homozygous.

Chemical compounds

KAR₁, KAR₂ and *rac*-GR24 were synthesized as previously reported (Goddard-Borger et al., 2007) . GR24^{5DS} and GR24^{ent-5DS} enantiomers were purified from *rac*-GR24 by chiral-phase HPLC as described (Scaffidi et al., 2014). 10 mM or 50 mM stocks were prepared in acetone and stored at -20°C, and freshly diluted in aqueous solutions before use.

Hypocotyl assay

Hypocotyl growth under red light was performed as described previously, but in a HiPoint DCI-700 LED Z4 growth chamber (Nelson et al., 2011). Surface-sterilized seeds were plated on 0.5x Murashige-Skoog (MS) media with 1 μM KAR₂, 1 μM *rac*-GR24, 0.5 μM GR24^{5DS}, 0.5 μM GR24^{ent-5DS} or 0.01% (v/v) acetone as mock control, stratified for 3 d at 4°C in darkness, treated with 3 h white light (~150 μmol m⁻²s⁻¹) at 21°C, returned to darkness for 21 h at 21°C, and then grown under continuous red light (~30 μmol m⁻²s⁻¹) at 21°C for 4 d before being photographed. Hypocotyl length was measured using ImageJ software (NIH).

Branching assay

The position of plants within flats was randomized to account for environmental variation. The number of primary rosette branches, not including the primary shoot, at least 1 cm in length was measured for each plant at global proliferative arrest (~7 weeks after germination).

RT-qPCR analysis

Total RNA was prepared and DNAse-treated with the Spectrum Plant Total RNA Kit and On-Column DNase I Digestion Set (Sigma-Aldrich) from non-elongated axillary buds collected 10 d after anthesis from plants grown in LD photoperiod. First-strand cDNA was synthesized from 2 μ g of total RNA with the iScript cDNA Synthesis Kit (Bio-Rad). Quantitative PCR was performed in a CFX384 Real-Time PCR Detection System (Bio-Rad) using Luna Universal qPCR Master Mix (NEB) with the following program: 5 min at 95°C and 45 cycles of 20 s at 95°C, 20 s at 60°C, and 20 s at 72°C, followed by melt curve analysis to analyze product specificity. The relative expression of *BRC1* was calculated by $2^{\Delta Cq}$ [$\Delta C_q = C_q(CACS) - C_q(BRC1)$]. Primers for *BRC1*, *RD29A*, *Cor15A*, *PKS5* and the *CACS* reference gene are previously described (Fujii et al. 2011; Wang et al. 2014; Soundappan et al., 2015).

Yeast Two-Hybrid Assay

To construct plasmids for yeast two-hybrid assays, cDNA sequences for *D14*, *d14*^{seto}, and *d14*^{S97A} were cloned into pDONR221 Gateway entry vector by BP clonase reaction, sequence-verified, and recombined by LR clonase reaction into Gateway yeast expression vector pDest-GBKT7 to generate BD-D14, BD-d14^{seto}, and BD-d14^{S97A}, respectively. To make GAL4 DNA activation domain (AD) constructs, the coding sequences for *SMAX1*, *SMXL2*, *SMXL7*, *SMAX1*_{D1M} and *SMXL7*_{D1M} were cloned into pDONR221, sequence-verified, and moved into Gateway yeast expression vector pDest-GADT7. Direct interaction of two proteins was investigated by co-transformation of the respective plasmids in the yeast strain Y2HGold (Clontech) by the standard

lithium acetate-mediated method (Gietz and Woods, 2002). The transformed yeast strains were plated on SD/-Leu-Trp medium (Clontech) at 30°C for 3 d. Interactions in yeast were tested on SD/-Leu-Trp-His and SD/-Leu-Trp-His-Ade (Clontech) medium supplemented with 2 μ M GR24^{5DS} or 0.02% (v/v) acetone.

Transient Expression in Nicotiana benthamiana

N. benthamiana plants (3 weeks old) were used to express the various construct combinations by Agrobacterium (GV3101 pMP90)—mediated transient transformation of lower epidermal leaf cells as described previously (Khosla et al., 2020a).

FRET-ABP assay

N. benthamiana leaves were sprayed with 10 µM estradiol 24 hours after infiltration of Agrobacterium to induce protein expression from LexA:SMXL7:mCherry (pAB118), LexA:SMAX1:mCherry LexA:SMXL7:mCherry-GFP (pAB118), (pAB119) LexA:SMAX1:mCherry-GFP. The assay was performed 24 h after induction on a Leica TCS SP5 laser scanning confocal microscope with a 63 x/ 1.2 NA water immersion objective. The FRET-APB wizard of LAS-AF was used with the following parameters: acquisition speed 700 Hz; pinhole 60.7 µm; image format 512 x 512 pixels; zoom 6X. Regions Of Interest (ROIs) of 6 x 3.5 µm were photobleached with 10 repeated exposures (laser 561 nm, 100% power level). Images were processed using Leica the Application Suite Advanced Fluorescence software (LAS-AF). FRET Efficiency (E_{FRET}%) was measured as the increase of donor fluorescence (GFP) intensity after photobleaching of the acceptor (mCherry). $E_{FRET}\% = 100 * (D_{post} - D_{pre}) / D_{post}$. D_{pre} and D_{post} were the fluorescence intensity of the donor before and after photobleaching, respectively, which were quantified using a secondary ROI inside the bleached region of the bleached region of the first ROI.

Degradation assays in N. benthamiana

To generate ratiometric reporter constructs for degradation assays in *N. benthamiana*, D14, d14^{seto}, and d14^{S97A}, SMAX1, SMXL2, and SMAX1_{D2} entry clones were transferred into the pRATIO1212 destination vector by Gateway LR reaction (Khosla et al., 2020a). To examine the time course of degradation, the wells of a black 96-well polystyrene plate (Corning Costar®) were filled with 200 µl chemical treatments (10 µM KAR₁, 10 μM GR24^{5DS}, 10 μM GR24^{ent-5DS}, or 0.02% (v/v) acetone). Leaf discs were excised 3 d post-infiltration and transferred to the treatment plate (one leaf disc per well) with the abaxial side up. Relative fluorescence was measured in a CLARIOstar plate reader (BMG Labtech) in plate mode (slow kinetics) at the indicated time points with the following settings: spiral scan option; scan diameter (mm), 5; and number of flashes per well per cycle, 36. Optimal settings for fluorescence measurements of the mScarlet-I reporter (ex. 560-10 nm, em. 595-10 nm) and Venus reference (ex. 497-15 nm, em. 540-20 nm) proteins were described previously (Khosla et al., 2020a). Degradation was quantified as mScarlet-I/Venus fluorescence intensity ratios after subtracting background fluorescence signals measured in leaf discs transformed with RNA silencing suppressor P19.

Degradation assays in Arabidopsis thaliana

4-day-old *35S:D14-GFP* and *35S:d14*^{seto}-*GFP* transgenic plants (Col-0 background) grown vertically were placed in a multiwell slide (1 μ-Slide, 8 wells IbiTreat, IBIDI) and immobilized with 200 μl of 0.5% (w/v) MS agar medium. The *rac*-GR24 was supplemented to a final concentration of 5 μM. Equivalent volume of acetone was added for mock control. 3 Z-series section images were captured every 10 min for 16 h at 22 °C with a Microfluor Leica DMI6000B fluorescence microscope using a 10x objective and 470 nm light to detect GFP. GFP signal was quantified with Fiji using Region of Interest (ROI) Multi Measure plugging after determining a threshold range to eliminate the background. The GFP signal variation of each plant over time was calculated as a percentage to the signal at t₀ when SL was just applied. Then we

obtained the relative GFP signal by normalizing the GFP signal to the mean of its mock control at each time point.

To monitor SMAX1_{D2}, SMXL7 or D14 degradation, 9-day-old plants expressing $35S:SMAX1_{D2}$ -LUC, UBQ:SMXL7-LUC or UBQ:D14-LUC grown on a white 96-well plate (Perkin Elmer OptiPlate 96) containing 200 µl 0.5x MS agar medium were sprayed with 2 mM D-luciferin and incubated 3 h before treatment to equilibrate. 5 µM GR24^{5DS}, 5 µM KAR₂, 300 mM mannitol, or corresponding solvent control were then sprayed along with 2 mM D-luciferin. Luciferase signal was measured using a CLARIOstar plate reader (BMG Labtech) under controlled 21°C temperature. The luciferase activity (LA) of each plant at each time point was calculated relative to time zero as LA (%) = [(cps_{tn} * 100) / cps_{t0}]. Then we obtained the Relative Luciferase Activity (RLA) by normalizing LA of each treatment/genotype to the average of corresponding solvent control at each time point.

Osmotic stress tolerance assays

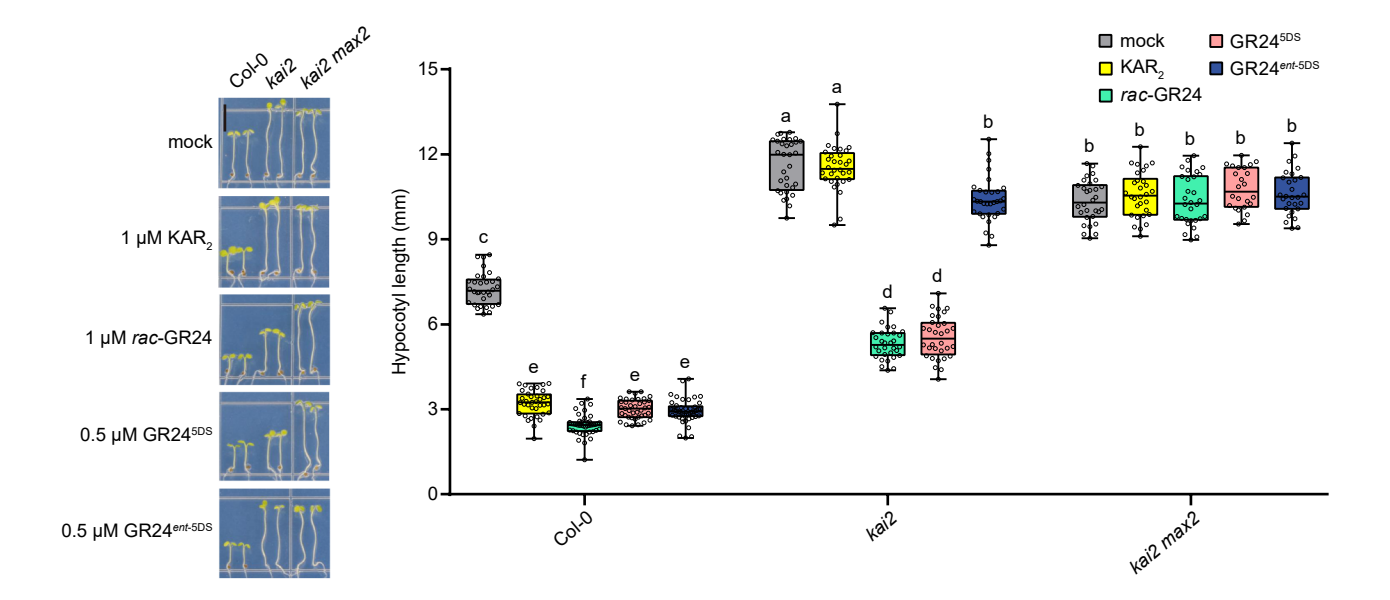
7-day-old seedlings grown on 0.5x MS agar were transplanted to 0.5x MS agar containing 300 mM mannitol to induce osmotic stress. Seedlings were photographed and assayed after 14 d mannitol treatment. The aerial parts of 3-5 seedlings were excised and weighed. Tissues were ground by a bead mill and homogenized in extract solution (95% ethanol + 5% water) at 4 °C overnight until bleached. The total chlorophyll content was quantified by measuring the absorbance of the supernatant at 647 and 665 nm and using the formula total Chl = (17.90 * A_{647} + 8.08 * A_{665})/mg fresh weight (Chen et al., 2013).

Statistical analysis

Data were analyzed by using JMP Pro 13 and Excel. For multiple comparisons of means, one-way ANOVA was performed followed by Tukey's HSD test (p < 0.05) or Student's t-test (p < 0.05). Two-sided Student's t-test was conducted for comparisons of

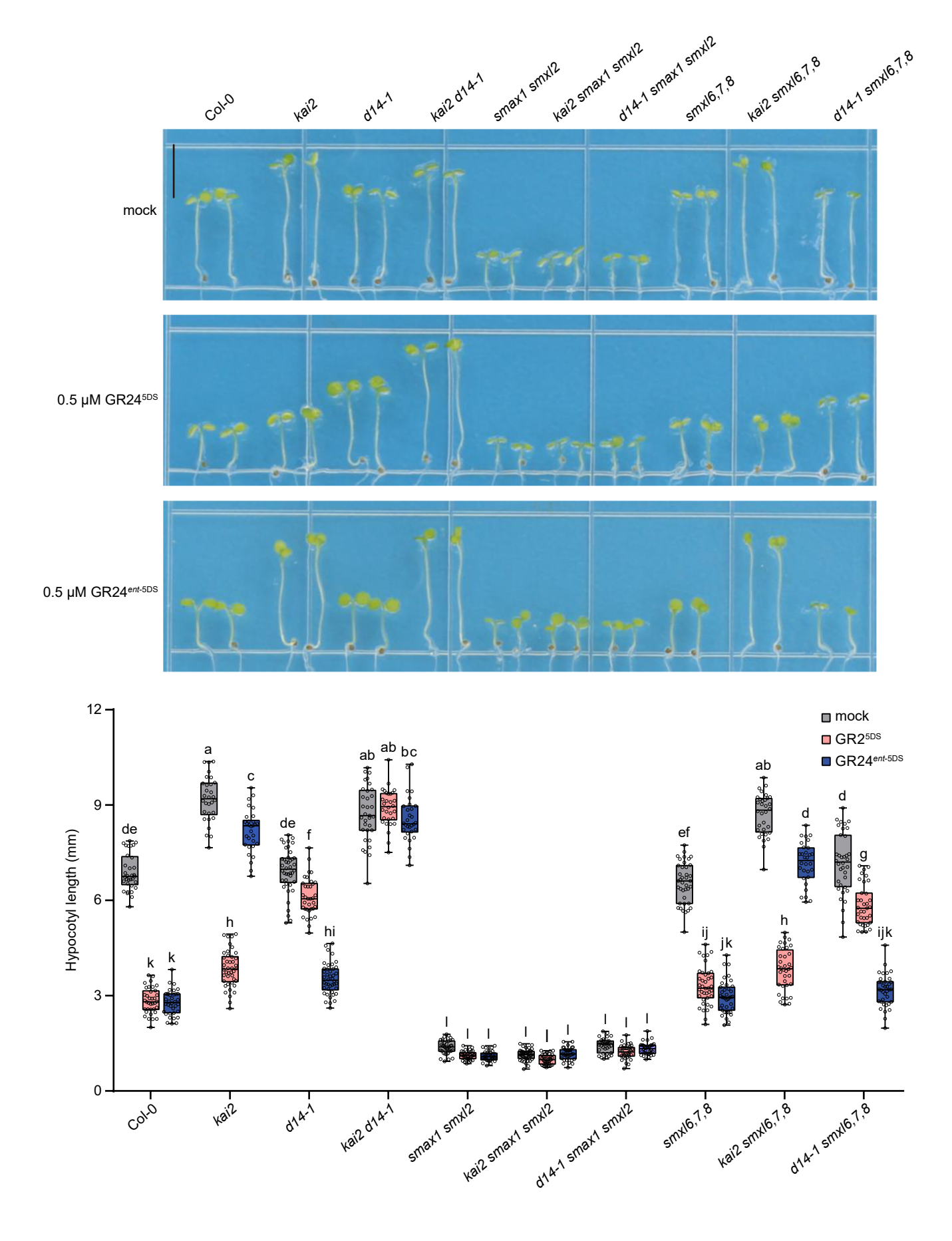
means between two groups. Graphs were produced using Prism v7 (GraphPad Software). Box plots show the median, 25th percentile, and 75th percentile. Whiskers indicate the minimum and maximum of the data range, and individual data points are overlaid. For sample sizes with $n \le 4$, individual data points and the mean value are shown.

- Chen, L.-J., Wuriyanghan, H., Zhang, Y.-Q., Duan, K.-X., Chen, H.-W., Li, Q.-T., Lu, X., He, S.-J., Ma, B., Zhang, W.-K., et al. (2013). An S-domain receptor-like kinase, OsSIK2, confers abiotic stress tolerance and delays dark-induced leaf senescence in rice. *Plant Physiol.* **163**:1752–1765.
- **Clough, S. J., and Bent, A. F.** (1998). Floral dip: a simplified method for Agrobacterium-mediated transformation of Arabidopsis thaliana. *Plant J.* **16**:735–743.
- **Fujii**, **H.**, **Verslues**, **P. E.**, **and Zhu**, **J.-K.** (2011). Arabidopsis decuple mutant reveals the importance of SnRK2 kinases in osmotic stress responses in vivo. *Proc. Natl. Acad. Sci. U. S. A.* **108**:1717–1722.
- Khosla, A., Rodriguez-Furlan, C., Kapoor, S., Van Norman, J. M., and Nelson, D. C. (2020a). A series of dual-reporter vectors for ratiometric analysis of protein abundance in plants. *Plant Direct* 4.
- Scaffidi, A., Waters, M. T., Sun, Y. K., Skelton, B. W., Dixon, K. W., Ghisalberti, E. L., Flematti, G. R., and Smith, S. M. (2014). Strigolactone Hormones and Their Stereoisomers Signal through Two Related Receptor Proteins to Induce Different Physiological Responses in Arabidopsis. *Plant Physiol.* 165:1221–1232.
- Soundappan, I., Bennett, T., Morffy, N., Liang, Y., Stanga, J. P., Abbas, A., Leyser, O., and Nelson, D. C. (2015). SMAX1-LIKE/D53 Family Members Enable Distinct MAX2-Dependent Responses to Strigolactones and Karrikins in Arabidopsis. *Plant Cell* 27:3143–3159.
- Wang, X.-H., Li, Q.-T., Chen, H.-W., Zhang, W.-K., Ma, B., Chen, S.-Y., and Zhang, J.-S. (2014). Trihelix transcription factor GT-4 mediates salt tolerance via interaction with TEM2 in Arabidopsis. *BMC Plant Biol.* 14:339.

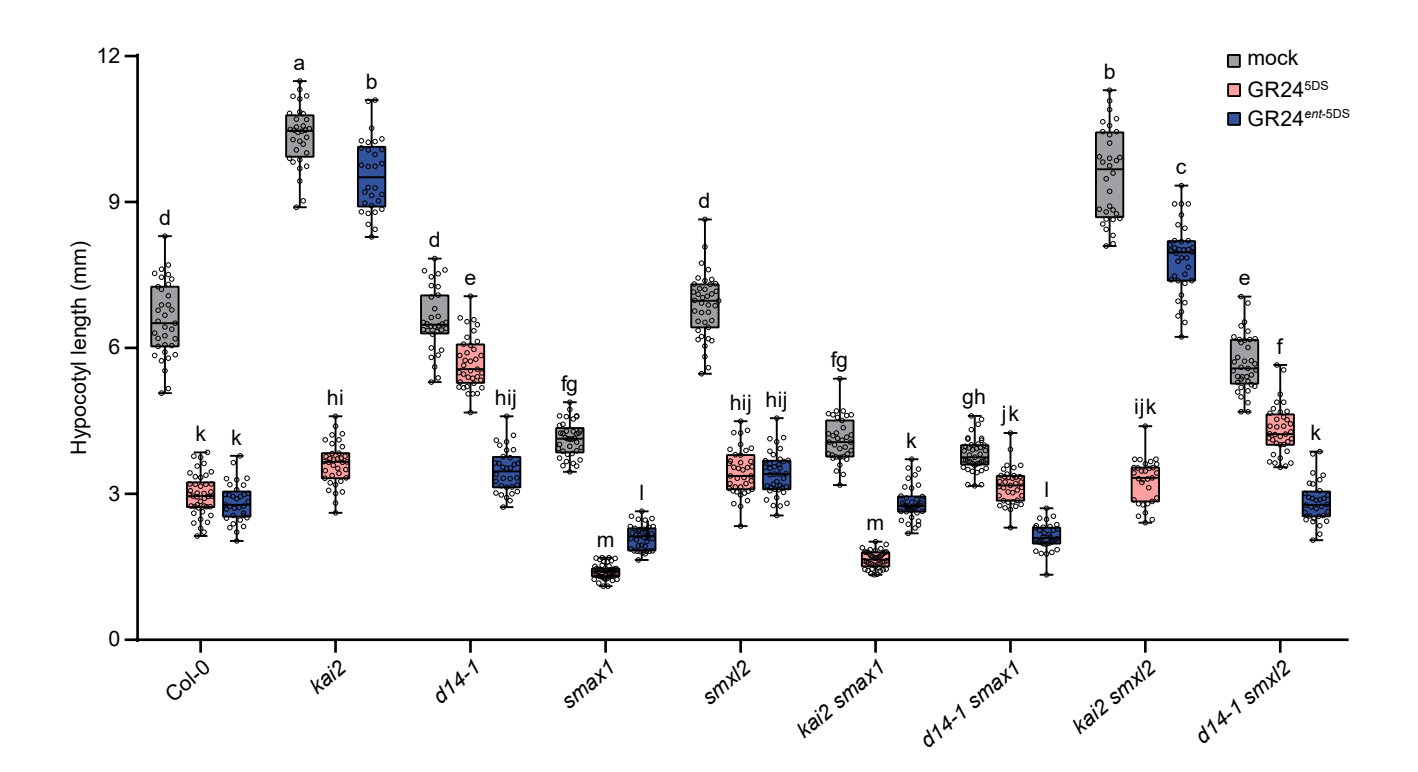


Supplemental Figure 1. Hypocotyl elongation of *kai2* is inhibited by *rac-*GR24 and GR24^{5DS} through *MAX2*.

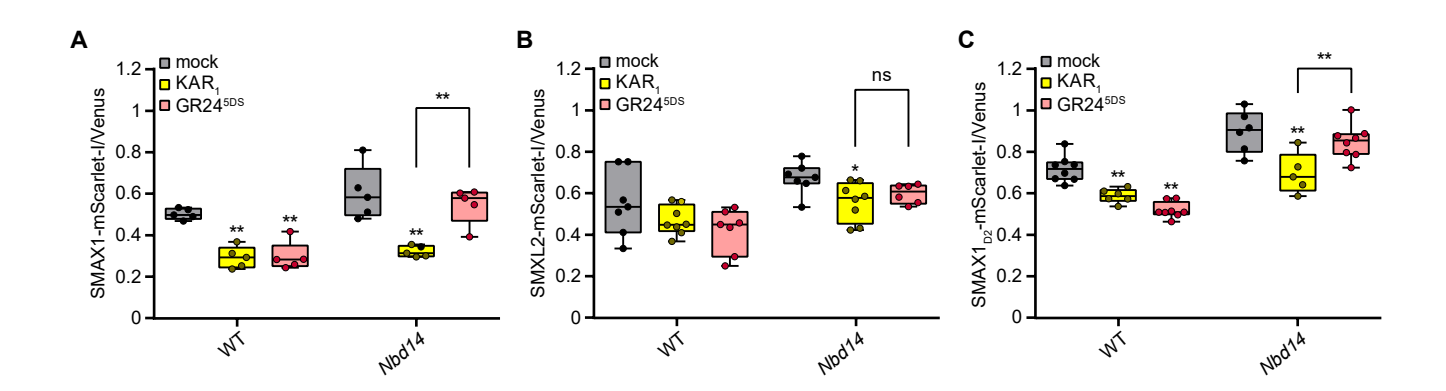
Hypocotyl length of 5-d-old seedlings of Col-0, kai2, and kai2 max2 are grown under continuous red light for 4 d on the 0.5x MS agar media containing 1 μ M KAR₂, 1 μ M rac-GR24, 0.5 μ M GR24^{5DS}, 0.5 μ M GR24^{ent-5DS} or acetone. Bar = 5 mm. Box-and-whisker plots with the same letter are not significantly different from one another (Tukey HSD, p < 0.05, n ≥ 30).



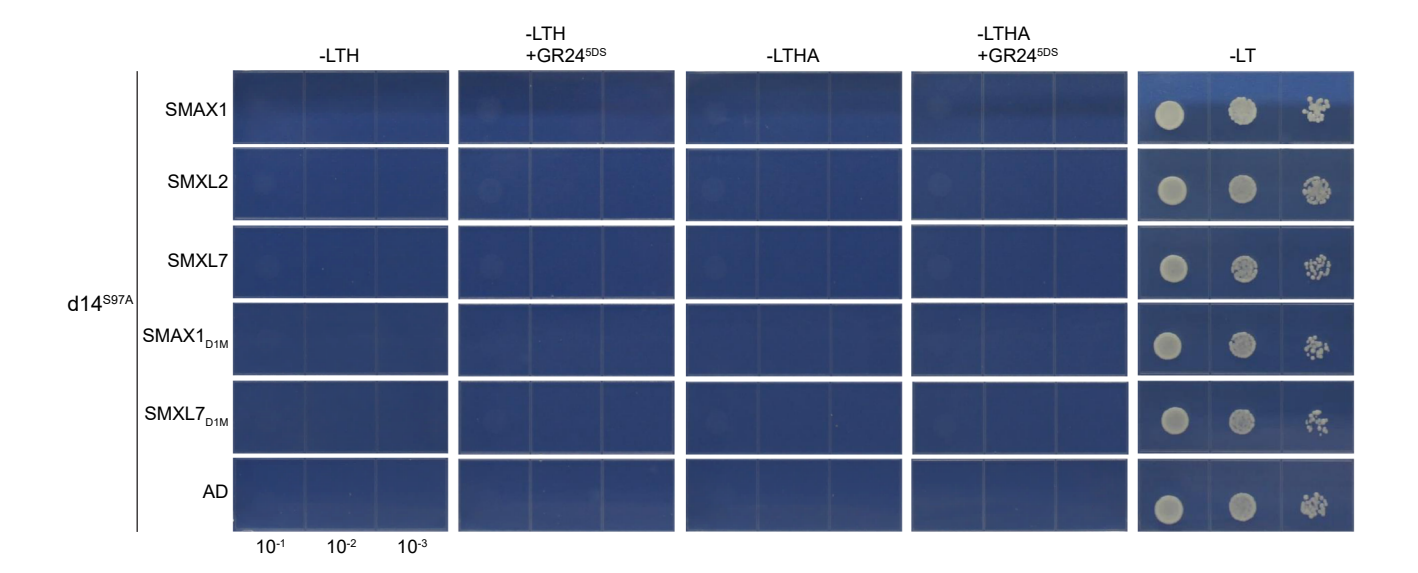
Supplemental Figure 2. Hypocotyl growth of plant materials in Figure 1 with GR24^{5DS} or GR24^{ent-5DS} treatment. 5-d-old seedlings of Col-0, kai2, d14-1, kai2 d14-1, smax1 smxl2, kai2 smax1 smxl2, d14-1 smax1 smxl2, smxl6,7,8, kai2 smxl6,7,8 and d14-1 smxl6,7,8 are grown under continuous red light for 4 d on the 0.5x MS agar media containing 0.5 μ M GR24^{5DS}, 0.5 μ M GR24^{ent-5DS} or acetone. Mock-treated seedling data are duplicated in Figure 1, which shows additional data from this experiment. Bar = 5 mm. Box-and-whisker plots with the same letter are not significantly different from one another (Tukey HSD, p < 0.05, n ≥ 30).



Supplemental Figure 3. Hypocotyl growth of plant materials in Figure 2 with GR24^{5DS} or GR24^{ent-5DS} treatment. 5-d-old seedlings of Col-0, kai2, d14-1, smax1, smxl2, kai2 smax1, d14-1 smax1, kai2 smxl2, d14-1 smxl2 are grown under continuous red light for 4 d on the 0.5x MS agar media containing 0.5 μ M GR24^{5DS}, 0.5 μ M GR24^{ent-5DS} or acetone. Mock-treated seedling data are duplicated in Figure 2, which shows additional data from this experiment. Box-and-whisker plots with the same letter are not significantly different from one another (Tukey HSD, p < 0.05, n ≥ 30).

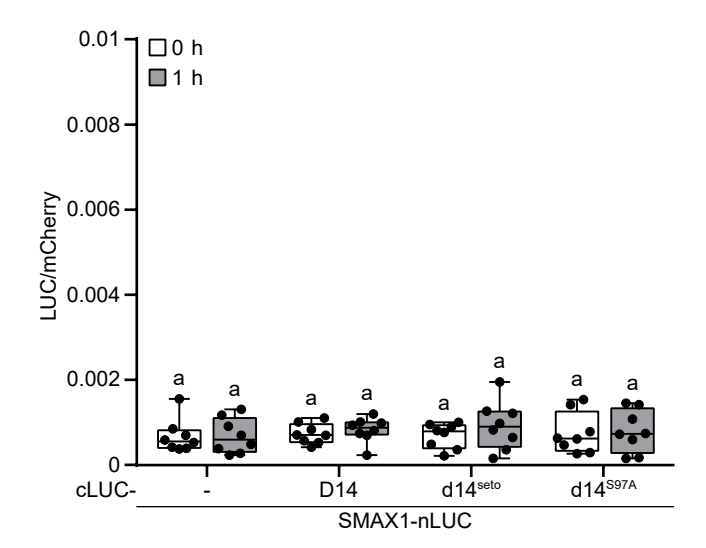


Supplemental Figure 4. Degradation of SMAX1, SMXL2 or SMAX1 $_{D2}$ after 4 h treatment of KAR $_1$ or GR24 5DS . Relative fluorescence from the SMAX1-mScarlet-I reporter (A) or SMXL2-mScarlet-I reporter (B) or SMAX1 $_{D2}$ -mScarlet-I reporter (C) and the Venus reference after transient expression of the ratiometric system in wt tobacco and *Nbd14* is shown. Leaf discs are treated with acetone, 10 μ M KAR $_1$, or 10 μ M GR24 5DS for 4 h. Mock-treated seedling data are duplicated in Figure 3A to 3C, which show additional data from this experiment. n = 5-8 leaf discs. ns indicates no significance. *p < 0.05, **p < 0.01, student's t test comparisons to the relative fluorescence at 0 h or between compared pairs.



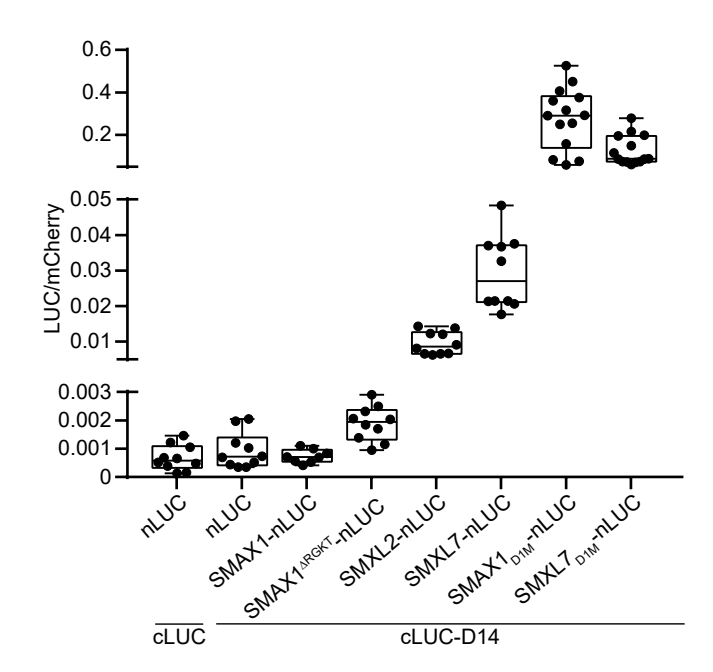
Supplemental Figure 5. Yeast two-hybrid assays for d14^{S97A} interactions with SMAX1, SMXL2, SMXL7, SMAX1_{D1M} and SMXL7_{D1M}.

and SMXL7_{D1M}. The d14^{S97A} is fused to GAL4-BD. SMAX1, SMXL7 and their D1M domains are fused to GAL4-AD. Serial 10-fold dilutions of yeast cultures are spotted onto selective growth medium (-L, -Leu; -T, -Trp; -H, -His; -A, -Ade) that is supplemented with 2 μ M GR24^{5DS} or acetone.



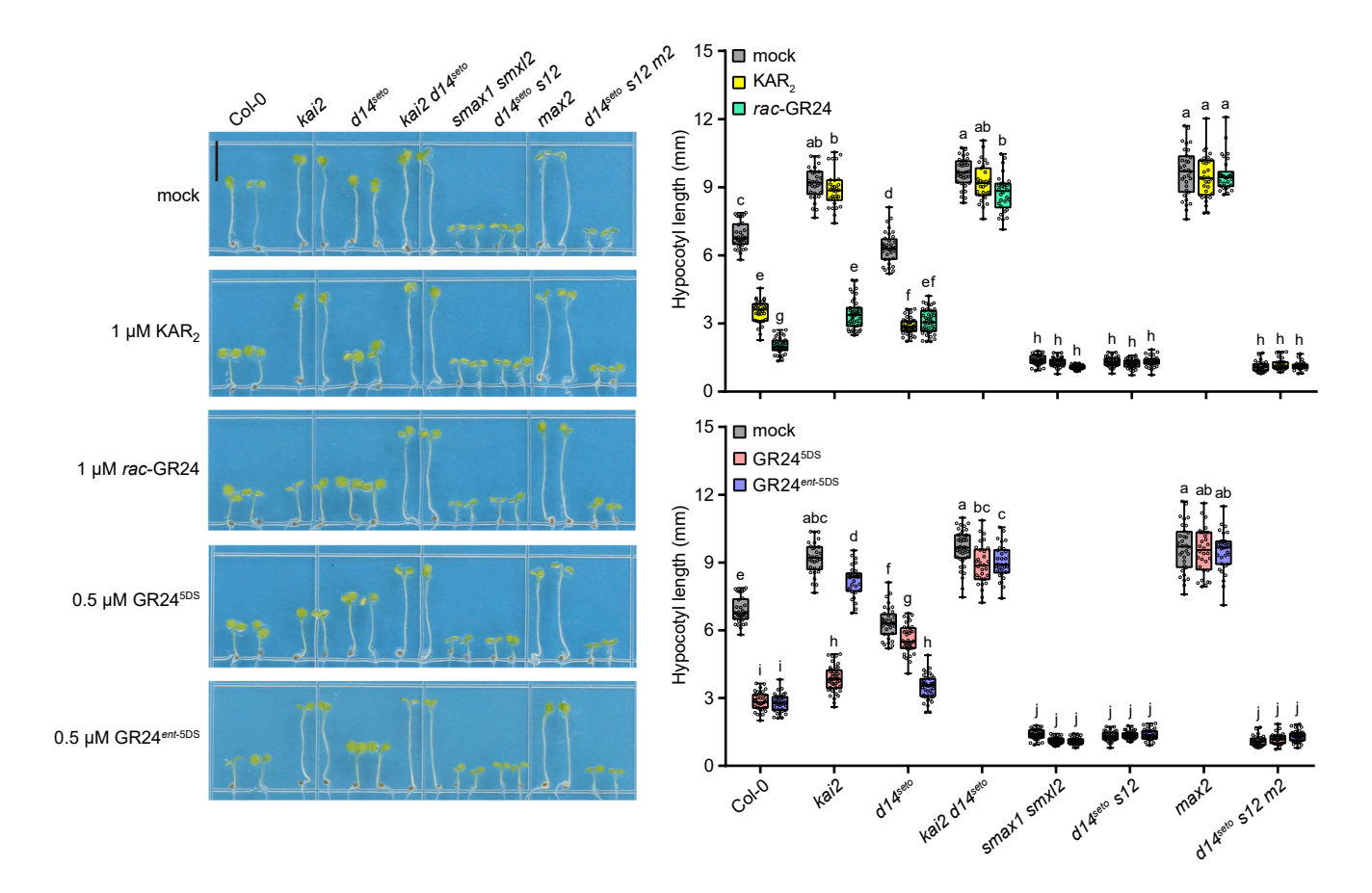
Supplemental Figure 6. D14, d14^{seto} and d14^{S97A} interactions with SMAX1 in split-luciferase assay.

N. benthamiana leaves are transiently co-transformed with $Agrobacterium\ tumefaciens$ strains carrying cLUC, nLUC, or indicated fusions as well as a strain carrying an mCherry transgene as a transformation control. Luminescence is measured before and 1 hour after treatment with 10 μ M GR24^{5DS}, and normalized against mCherry fluorescence. Box-and-whisker plots with the same letter are not significantly different from one another (n = 8 leaf discs).



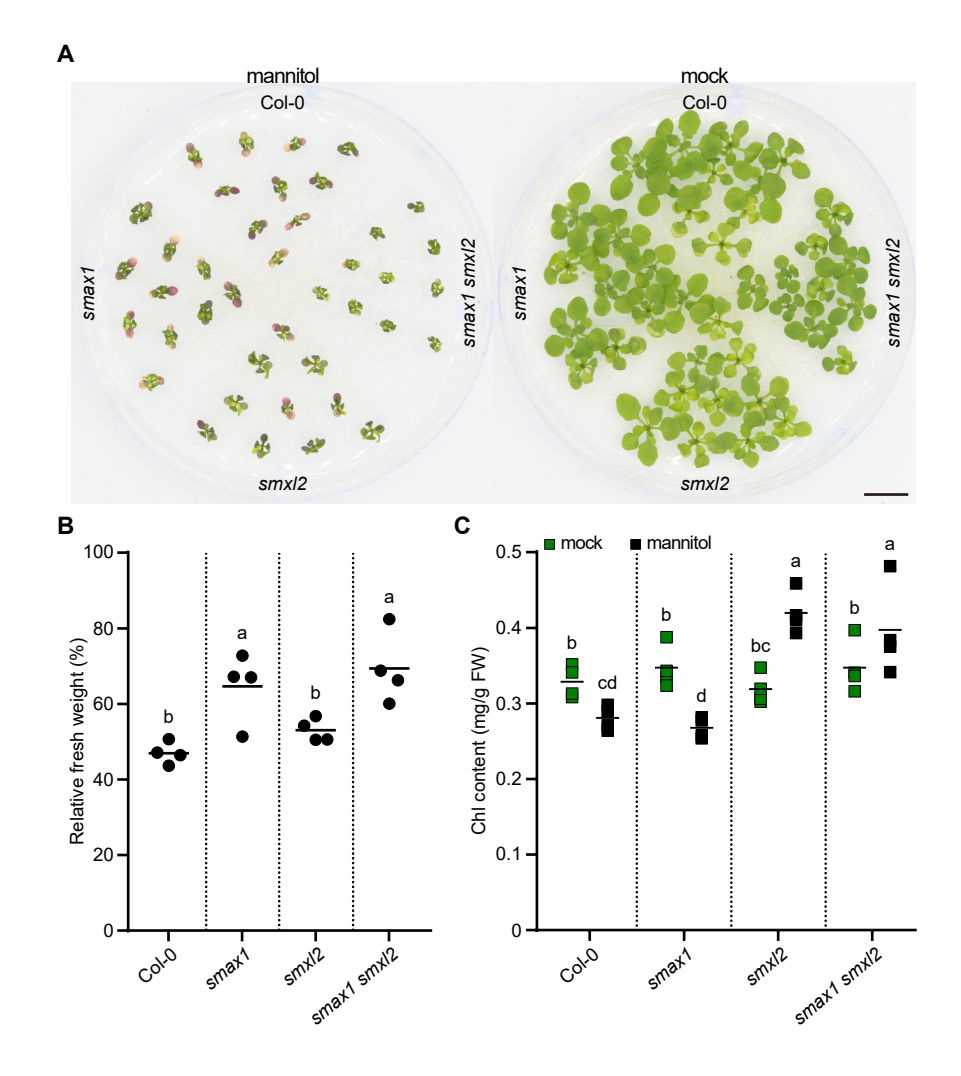
Supplemental Figure 7. Baseline of D14 interactions with SMAX1, SMXL2, SMXL7, SMAX1_{D1M} and SMXL7_{D1M} in split-luciferase assay.

N. benthamiana leaves are transiently co-transformed with *Agrobacterium tumefaciens* strains carrying cLUC, nLUC, or indicated fusions as well as a strain carrying an mCherry transgene as a transformation control. Luminescence is measured before 10 μ M GR24^{5DS} treatment, and normalized against mCherry fluorescence. n = 7-15 leaf discs. The data are duplicated in Figure 4B to 4F, which show additional data from this experiment.



Supplemental Figure 8. Hypocotyl growth of Col-0 (wild type), *kai*2, *d14*^{seto}, *kai*2 *d14*^{seto}, *smax*1 *smxl*2, *d14*^{seto} *smax*1 *smxl*2, *max*2, *d14*^{seto} *smax*1 *smxl*2 max2 under different treatments.

Plants are grown under continuous red light for 4 d on the 0.5x MS agar media containing 1 μ M KAR₂, 1 μ M rac-GR24, 0.5 μ M GR24^{5DS}, 0.5 μ M GR24^{ent-5DS} or acetone. Bar = 5 mm. Box-and-whisker plots with the same letter are not significantly different from one another (Tukey HSD, p < 0.05, n ≥ 30).

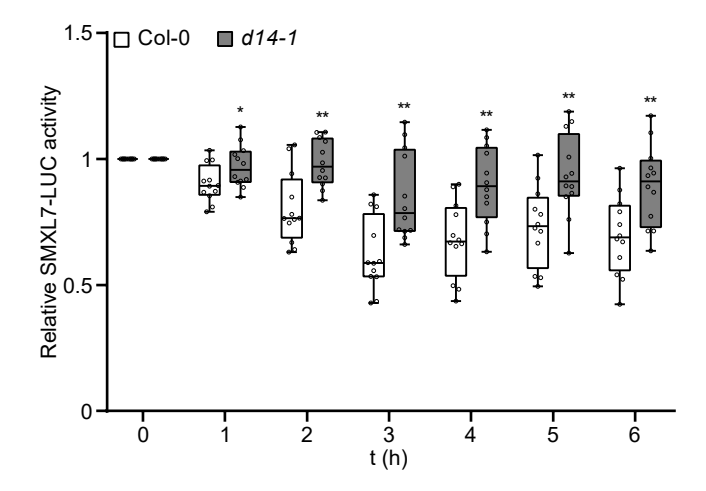


Supplemental Figure 9. Osmotic stress tolerance of Col-0, smax1, smxl2 and smax1 smxl2.

(A) 21-day-old seedlings of Col-0, *smax1*, *smxl2* and *smax1 smxl2* grown in mock or 300 mM mannitol condition for 14 days. Bar = 1 cm.

(B) Relative fresh weights of plant materials used in **(A)** to application of 300 mM mannitol. The weights of aerial parts from plants grown on 0.5x MS agar medium containing 300 mM mannitol are scaled to that from plants grown on 0.5x MS agar medium. Scatter dot plots with the same letter are not significantly different from one another (bar indicates mean; n = 4; student's t, p < 0.05).

(C) Chlorophyll (Chl) contents in the aerial parts of Arabidopsis seedlings used in (A). Others are as in (B).



Supplemental Figure 10. Osmotic stress triggers the SMXL7 degradation.

Bioluminescence of SMXL7-LUC in Col-0 and d14-1 backgrounds. Seedlings were treated with 300 mM mannitol or water control. Bioluminescence is shown as relative LUC activity and is monitored for 6 h after treatment. n = 12 seedlings. *p < 0.05, **p < 0.01, student's t test comparisons to Col-0 control at each time point.



Supplemental Figure 11. Rosette phenotypes of plant materials in Figure 5A.
Col-0 (wild type), d14-1, kai2 d14-1, d14-1 smax1, d14-1 smax1 smxl2, d14^{seto}, kai2 d14^{seto}, d14^{seto} smax1, d14^{seto} smax1 smxl2, max2 and d14seto smax1 smxl2 max2 are grown for 4 weeks under a long-day photoperiod (16 h light/8 h dark) before imaging. Bar = 5 cm.

Supplemental Table 1. Primers used in this study.

Primers for genotyping kai2-F CACTTGGTTCCACATCTGGTC kai2-R GAGATTTGAGTAACGATCGAAGTCG max2-1_dCAPS-F TGTCCGAATTTGGAAGAGATTAGG max2-1_dCAPS-R CAAGAAGAATCTTTCCCATAAACTCGAAT d14-1-WiscLoxHS-LP AAGAATATGGCAAGTGCAAC L4 WiscLoxHS TGATCCATGAGATTTCCCGGACATGAAG	
kai2-R GAGATTTGAGTAACGATCGAAGTCG max2-1_dCAPS-F TGTCCGAATTTGGAAGAGATTAGG max2-1_dCAPS-R CAAGAAGAATCTTTCCCATAAACTCGAAT d14-1-WiscLoxHS-LP AAGAATATGGCAAGC d14-1-WiscLoxHS-RP GATGATTCCGATCATAGCG	
max2-1_dCAPS-F TGTCCGAATTTGGAAGAGATTAGG max2-1_dCAPS-R CAAGAAGAATCTTTCCCATAAACTCGAAT d14-1-WiscLoxHS-LP AAGAATATGGCAAGT d14-1-WiscLoxHS-RP GATGATTCCGATCATAGCG	
max2-1_dCAPS-R CAAGAAGAATCTTTCCCATAAACTCGAAT d14-1-WiscLoxHS-LP AAGAATATGGCAAGT d14-1-WiscLoxHS-RP GATGATTCCGATCATAGCG	
d14-1-WiscLoxHS-LP AAGAATATGGCAAGTGCAAC d14-1-WiscLoxHS-RP GATGATTCCGATCATAGCG	
d14-1-WiscLoxHS-RP GATGATTCCGATCATAGCG	
14 Wisel ov HS TGATCCATGTAGATTTCCCGGACATGAAG	
L4_WiscLoxHS TGATCCATGTAGATTTCCCGGACATGAAG	
smax1-2-Salk-LP GTGGCAACTGTTTAGGCTGAG	
smax1-2-Salk-RP AAGCTAGCTTTTCAAGTCCCG	
smxl6-4-Salk-LP AGCCAGAGAAAGACTCGAACC	
smxl6-4-Salk-RP TCCGAAATTAAGCTCGATGTG	
smxl8-1-Salk-LP GAATCACAAATTCTGCATGGC	
smxl8-1-Salk-RP CTGACGAAGCTCCACTTTCAC	
Salk-LBb1.3 ATTTTGCCGATTTCGGAAC	
smxl7-3-WiscDsLox-LP GATCAAGAAACGAACGCTGAG	
smxl7-3-WiscDsLox-RP CGTATTAGCCTCTCGGATTCC	
WiscDsLox-LB-p745 AACGTCCGCAATGTGTTATTAAGTTGTC	
smxl2-1-Sail-LP TGACATACACCGATCACCAC	
smxl2-1-Sail-RP GTATCATCCCACTTTGCATAC	
Sail-LB1 GCCTTTTCAGAAATGGATAAATAGC	
seto5_dCAPS-F GGAGGATTCGAAGAAGGTGAGATTG	
seto5_dCAPS-R CGTACGCATATTAAACAAAGTACGGC	
Primers for constructs	
D14-cLUC-F TCGTACGCGTCCCGGGGCATGAGTCAACACATCTTAGAA	
D14-cLUC-R CGAACGAAAGCTCTGCAGTCACCGAGGAAGAGCTCGCC	
SMAX1-nLUC-F AACACGGGGGACGAGCTCATGAGAGCTGGTTTAAGTACGAT	
SMAX1-nLUC-R GGACGCGTACGAGATCTGTACTGCCAAAGTAATAGTTGTCG	
SMXL2-nLUC-F GAGAGAACACGGGGGACGAGCTCATGAGAGCAGATTTGATTACTATACAGC	;
SMXL2-nLUC-R CCGGGACGCGTACGAGATCTG AACGACCACCGTCCTGATACTAC	
SMXL7-nLUC-F AACACGGGGGACGAGCTCATGCCGACACCAGTAACCACG	
SMXL7-nLUC-R GGACGCGTACGAGATCTGGATCACTTCGACTCTCGCCGG	
SMAX1 _{D1M} -nLUC-F GAGAGAACACGGGGGACGAGCTCATGTTACAACAGAACGCTTCGTC	
SMAX1 _{D1M} -nLUC-R CCGGGACGCGTACGAGATCTGGATGTTATTATTGTTCTGCACTGATTCAG	
SMXL7 _{D1M} -nLUC-F GAGAGAACACGGGGGACGAGCTCATGGACATTAAACTCGACGTGCTTCATC)
SMXL7 _{D1M} -nLUC-R CCGGGACGCGTACGAGATCTGTGGTTCTTCGATGCGTAG	
Primers for qRT-PCR	
BRC1-F TCGCGACAACCCTTTCTCACCAT	
BRC1-R CGGTCGTGTTAGTATTGCTGCCTCT	
RD29A-F GCCGACGGGATTTGACG	
RD29A-R GCCGACGGGATTTGACG	
Cor15A-F ATGGCGATGTCTTTCTCAGGAGCTGTT	
Cor15A-R TTTTATCCGTCACGAAATCTGAAGCTT	

PKS5-F	GTTTGCGAGAGAGGAATCTG
PKS5-R	CCACAAGCAAATCATTCAACCG
CACS-F	GGAGAAGAGGGCCTTGCTTACAA
CACS-R	TTAGCTGGGCGAGATTTCATTTCTG